Air-water fluxes and sources of carbon dioxide in the Delaware Estuary: Spatial and seasonal variability

A. Joesoef, W.-J. Huang*, Y. Gao, and W.-J. Cai

School of Marine Science and Policy, University of Delaware, Newark, Delaware, USA

*present address: Department of Oceanography, National Sun Yat-Sen University, Kaohsiung 804, Taiwan

Correspondence to: W.-J. Cai (wcai@udel.edu)

Abstract

Distributions of surface water partial pressure of carbon dioxide (pCO_2) were measured on nine cruises in the Delaware Estuary (USA). The Delaware River was highly supersaturated in pCO_2 with respect to the atmosphere during all seasons while the Delaware Bay was undersaturated in pCO_2 during spring and late summer and moderately supersaturated during mid-summer, fall, and winter. While the smaller upper tidal river was a strong CO_2 source (27.1 ± 6.4 mol-C m^{-2} yr^{-1}), the much larger bay was a weak source (1.2 ± 1.4 mol-C m^{-2} yr^{-1}), the latter of which had a much greater area than the former. In turn, the Delaware Estuary acted as a relatively weak CO_2 source (2.4 ± 4.8 mol-C m^{-2} yr^{-1}), which is in great contrast to many other estuarine systems. Seasonally, pCO_2 changes were greatest at low salinities ($0 \leq S < 5$) with pCO_2 values in the summer nearly three-fold greater than those observed in the spring and fall. Undersaturated pCO_2 was observed over the widest salinity range ($7.5 \leq S < 30$) during spring. Near to supersaturated pCO_2 was generally observed in mid- to high salinity waters ($20 \leq S < 30$) except during spring and late summer. Strong seasonal trends in internal estuarine production and consumption of CO_2 were observed throughout both the upper tidal river and lower bay. Comparably, positive correlations between river-borne and air-water CO_2 fluxes in the upper estuary emphasize the significance of river-borne CO_2 degassing to overall CO_2 fluxes. While river-borne CO_2 degassing heavily influenced CO_2 dynamics in the upper tidal river, these forces were largely compensated by internal biological processes within the extensive bay system of the lower estuary.

1 Introduction

While, globally, the surface area of estuaries is only about 4% that of continental shelves, recent studies have concluded that the carbon dioxide (CO_2) degassing flux from estuarine waters is as large as the CO_2 uptake by the continental shelf (Borges, 2005; Borges et al., 2005; Cai et al., 2006; Chen and Borges, 2009; Cai, 2011). Global estuarine waters are estimated to emit 0.10-0.45 Pg C yr^{-1} while continental shelves take up 0.20-0.40 Pg C yr^{-1} (Borges, 2005; Borges et al., 2005; Cai, 2011; Chen et al., 2013; Regnier et al., 2013; Laruelle et al., 2015). Such large estuarine CO_2 degassing suggests that much of the terrestrial organic carbon, including that from coastal wetlands, is respired to CO_2 during transport through the estuarine zone, though the relative importance of river supplied CO_2 and organic carbon versus those from the coastal

wetlands is debatable (Borges and Abril, 2011; Cai, 2011). In turn, estuarine waters are a major source of CO_2 to the atmosphere, with partial pressures of CO_2 (pCO_2) ranging from 350 to 10,000 µatm and air-water CO_2 fluxes ranging from -5 to 80 mol C m^{-2} yr^{-1} (Raymond et al., 1997; Cai and Wang, 1998; Frankignoulle et al., 1998; Borges, 2005; Borges et al., 2006; Borges and Abril, 2011; Cai 2011).

There is rising concern that global estuarine CO_2 degassing flux may be overestimated (Cai, 2011). Although substantial progress has been achieved over the past decade (Borges and Abril, 2011; Chen et al., 2013; references therein), our knowledge of CO_2 degassing fluxes and their controlling processes in estuaries remains insufficient. Globally, the majority of past estuarine CO_2 studies have been conducted on small estuarine systems, which typically have high pCO_2. (Chen and Borges, 2009; Cai, 2011; Borges and Abril, 2011). Specifically, in the U.S. east coast, high pCO_2 was found in estuaries along the southeastern (Cai and Wang, 1998; Jiang et al., 2008) and northeastern (Salisbury et al., 2008; Hunt et al., 2010) coastal regions. While high pCO_2 was also found in small estuaries along the U.S. Mid-Atlantic coast (Raymond et al., 1997; Raymond et al., 2000), only a few estuarine CO_2 studies have been conducted in this region, such as Crosswell et al., (2012) in the Neuse River, NC, Raymond et al., (1997) in Hudson River, NY, and Raymond et al., (2000) in the York River, VA. Thus, there is limited research on CO_2 dynamics in large estuaries or bay systems with long freshwater residence times in the U.S. Mid-Atlantic coast (most notably the Chesapeake and Delaware estuaries). Presumably, these large estuaries have lower pCO_2 than small estuaries or bay systems with rapid freshwater transit times (Borges and Abril, 2011; Cai, 2011). Except for a few recent studies and the pioneering work of Sharp and Culberson, over the past 30 years there have been few inorganic carbon studies in the Delaware Estuary (Culberson, 1988; Sharp, 2009). Air-water CO_2 fluxes, total DIC fluxes, and ongoing evaluations of water acidification have not been consistently (via annual and seasonal surveys) studied. Overall, there is a lack of data and pressing need to synthesize and expand global research to larger estuaries. Furthermore, of past estuarine CO_2 studies, many lack spatial and seasonal coverage of surface water pCO_2 and air-water CO_2 fluxes, making flux estimates highly uncertain.

The Delaware Estuary is composed of a 100-km-long tidal Delaware River and the Delaware Bay (Fig. 1) (Sharp, 2010). With a relatively simple hydrology, the Delaware Estuary is fairly easy to characterize, and because of this, it has served as a model estuary for biogeochemical

studies (Cifuentes et al., 1988; Sharp et al., 2009). The tidal freshwater portion of the Delaware River flows from the head of the tide near Trenton, NJ through the greater Philadelphia area, the sixth largest municipal region of the U.S., before passing into the saline Delaware Bay (Fig. 1) (Sharp et al., 2009; Sharp, 2010). In turn, the upper Delaware River is heavily influenced by major industrial activity and continuously responding to a rapidly changing environment. For example, in the mid-20th century, the urban river of the Delaware Estuary suffered from severe hypoxia with average summer dissolved oxygen (DO) concentrations near zero value (Sharp, 2010). Fortunately, the implementation of the Clean Water Act (CWA) in the early 1970s helped promote efforts to improve water quality conditions in the Delaware River. With major upgrades to large sewage treatment plants, DO concentrations since the early 1990s have consistently been above the CWA standard of 3.5 mg L^{-1} (~219 µmol L^{-1}) (Sharp, 2010). Nonetheless, high pCO_2 is still expected to associate with strong respiratory O_2 consumption in the upper estuary. In contrast, the Delaware Bay is a large shallow embayment surrounded by salt marshes with minimal industrial or municipal inputs (Cifuentes et al., 1988). Thus, the Delaware Estuary is governed by the dynamic interaction between a river-dominated upper estuary and an ocean-dominated lower bay. This feature, typical for other large estuaries, and depending on river flow and geomorphology, smaller estuarine systems as well, provides us the opportunity to examine how contrasting geographical settings, physical mixing processes, and ecosystem metabolism in an extensive bay system can affect CO_2 gas exchange.

In this paper, we report the first seasonal distribution of pCO_2 and air-water CO_2 flux in the Delaware Estuary, which was surveyed nine times via various day- to week-long surveys from 2013 through 2014. We further assess the temperature and biological effects on pCO_2 distributions as well as the overall contribution of internal versus riverine sources on CO_2 inputs to the estuarine system. Finally, we present a summarized pCO_2 distribution over the study area and provide a conceptual model to illustrate the control mechanisms on surface water CO_2 dynamics in the Delaware Estuary.

2 Methods

2.1 Field measurements

The Delaware Estuary was surveyed on nine cruises: 08-10 June 2013, 08-15 August 2013, 17 October 2013, 17-22 November 2013, 23-24 March 2014, 03 July 2014, 27 of August to 01 of

September 2014, 30 of October to 02 November 2014, and 05 December 2014. Distributions of pCO_2, dissolved inorganic carbon (DIC), total alkalinity (TA), and pH were measured from the mouth of the bay to the near zero salinity of the estuary in five of the nine cruises. During the August and October 2013 cruises, only surface water pCO_2 was measured.

To monitor levels of pCO_2, surface water was directly pumped from 1 to 2 meters below the sea level through an underway pCO_2 analyzer (AS-P2, Apollo Scitech) installed in the shipboard laboratory (Huang et al., 2015). Surface water flowed into a 1 L volume shower head equilibrator at a minimum rate of 1.7 L min^{-1} to facilitate rapid gas exchange. A specifically designed water-drain system is attached to the equilibrator to insure that the pressure inside and outside remains balanced (Jiang et al., 2008b). The equilibrated gas was pumped through a water trap (Peltier cooler), which removed most of the water vapor, and then into a drying tube packed with magnesium perchlorate [$Mg(ClO_4)_2$] or Nafion tubing. Surface water CO_2 (mole fraction of dry air [xCO_2]) was measured approximately every one and a half minutes using an underway flow-through system equipped with a non-dispersive infrared (NDIR) gas analyzer (Li-Cor Model Li-7000, Lincoln, NE, USA). This LICOR 7000 was calibrated, every 3-6 hours, against three or four CO_2 gas standards (151.5, 395.4, 982.6, and 1969 ppm CO_2 in air) referenced against standards traceable to those of the National Institute of Standards and Technology (NIST). Atmospheric xCO_2 was measured every 3-6 hours using the same CO_2 system. In order to avoid contamination from the ship's stack gases or other possible sources of air pollution, the inlet of the atmospheric CO_2 pipe was installed on the highest platform in the front of the ship. An on-board Sea-bird thermosalinograph (SBE-45) measured surface water temperature and salinity. To calculate surface water and atmospheric pCO_2 values, all xCO_2 measurements were corrected to 100% saturation of water vapor pressure and the in situ surface water temperature (Dickson et al., 2007).

DIC and TA water samples were collected throughout the salinity gradient. Multiple samples were taken at near salinity zero and at the mouth of the bay to obtain river and ocean end-member values. Samples for DIC and TA measurements were filtered through a cellulose acetate filter (0.45 μm) into 250 ml borosilicate bottles and then fixed with 100 μl of saturated mercury bichloride solution (Cai and Wang, 1998; Jiang et al., 2008a). When collecting water, all bottles were overflowed for at least twice its volume to minimize contact with the atmosphere. Afterwards, sample bottles were kept in 4 to 10°C for future analysis. DIC was determined by

acidifying 0.5-1.0 ml samples with phosphoric acid. The extracted CO_2 gas was subsequently quantified via an infrared gas analyzer (AS-C3 Apollo Scitech). TA was measured by Gran titration (Gran, 1952) using the open cell method with a semi-automatic titration system (AS-ALK2, Apollo Scitech) (Cai et al., 2010a; Huang et al., 2012). Both DIC and TA measurements were calibrated against certified reference material (CRM, provided by A.G. Dickson from Scripps Institution of Oceanography) at a precision level of about ± 2 μmol kg^{-1} (Huang et al., 2012).

2.2 Air-water CO_2 flux estimation

In this study, air-water CO_2 fluxes (F, mmol m^{-2} d^{-1}) at pixel i of a 0.01 longitude x 0.01 latitude grid were calculated as follows:

$$F_i = k_i \cdot K_{oi} \cdot (pCO_{2(water)i} - pCO_{2(air)i}) \quad (1)$$

where k_i (cm h^{-1}) is the gas transfer velocity of CO_2, K_{oi} is the solubility coefficient of CO_2 (mol L^{-1} atm^{-1}), which can be calculated from in situ temperature and salinity (Weiss, 1974), and $pCO_{2(water)i}$ and $pCO_{2(air)i}$ (μatm) are the partial pressure of CO_2 in the water and the air, respectively. The mean atmospheric xCO_2 during each cruise and the sea surface temperature, salinity, and pressure were used to calculate the $pCO_{2(air)i}$. A positive F value indicates CO_2 transfer from water to the atmosphere.

Generally, two main issues arise when trying to accurately determine air-water CO_2 fluxes in coastal waters: how to accurately represent surface turbulence and obtaining spatial and temporal heterogeneity of pCO_2 distributions. One of the greatest uncertainties when calculating air-water CO_2 fluxes is estimating gas transfer velocities (Wanninkhof et al., 2009). While gas transfer velocities primarily depend on wind regime in the open ocean, in coastal and shallower estuaries it is probably more complicated as other factors such as tidal currents, bottom stress, wave slope, turbidity, surface films, and fetch limitation can also influence gas exchange rates (Raymond and Cole, 2001; Borges et al., 2004; Zappa et al., 2007; Jiang et al., 2008a; Abril et al., 2009). Unfortunately, because there have not been many studies on gas transfer velocities in estuaries, we relied on wind speed dependence to estimate gas exchange rates. Moreover, limited research has been conducted at wind speeds less than 4 m s^{-1}. In turn, quadratic relationships that estimate k often extrapolate to zero at low wind speeds (Wanninkhof et al., 2009). Increasing evidence suggests that k does not approach zero at low wind speeds but rather asymptotes to a finite value due to various external factors such as buoyancy effects, chemical enhancements, and physical

mixing processes (McGillis et al., 2001; McGillis et al., 2004; Wanninkhof et al., 2009). To avoid gas transfer velocities of zero in river and inland waters where wind speeds are typically low, we adopted the gas transfer relationship as proposed by Wanninkhof et al., (2009):

$$k_{660} = 3 + 0.1 \cdot U_{10} + 0.064 \cdot U_{10}^2 + 0.011 \cdot U_{10}^3 \quad (2)$$

where k_{660} is the gas transfer velocity at the Schmidt number of 660, which can be calculated from in situ sea surface temperature (Wanninkhof, 1992), and U_{10} is the wind speed at 10 meters above the water surface. Another challenge to accurately determining air-water CO_2 fluxes is obtaining reliable spatial and temporal pCO_2 distributions. Unfortunately, while seasonal distributions of pCO_2 were measured from the mouth of the bay to near zero salinity of the estuary (north to south), our lack of cross bay transects (east to west) limits our knowledge of CO_2 dynamics in shallow water regions of the estuary. Thus, there is a pressing need to conduct more research near these shallow water boundaries.

In addition, because the relationship between k and mean wind speeds is nonlinear, temporal distributions of wind speeds influence gas transfer velocities (Wanninkhof, 1992; Wanninkhof et al., 2002). To accurately determine the effect of variability of winds over a month, Wanninkhof (1992) introduced the nonlinearity coefficient of the wind speeds (C_2), which is calculated as follows (Wanninkhof et al., 2002; Jiang et al., 2008b):

$$C_2 = \left(\frac{1}{n}\sum_{j=1}^{n} U_j^2\right)/U_{mean}^2 \quad (3)$$

where C_2 is the nonlinearity coefficient for quadratic terms of gas transfer relationships, U_j is the high-frequency wind speed collected at the buoys, U_{mean} is the monthly mean wind speed, and n is the total number of available wind speeds during that month. We used high-frequency wind speed data (measured every six minutes) obtained from four National Oceanic and Atmospheric Administration (NOAA) buoys (LWSD1, CMAN4, SJSN4, and DELD1) to calculate the nonlinearity coefficients at each buoy and extrapolate them to the entire estuary. Using the calculated nonlinearity coefficients, gas transfer relationships were corrected to obtain the most accurate relationship between gas transfer velocities and wind speeds during each month.

In order to calculate area-averaged CO_2 flux throughout the Delaware Estuary, the system was divided into five geographic zones as defined by Sharp et al. (2009). However, due to rapid change in pCO_2 values across the mid-bay, this region was split into an upper and mid-bay zone to allow for a more robust comparison of pCO_2 and CO_2 fluxes throughout the system (Fig. 1). Surface water pCO_2, temperature, salinity, wind speed, and pressure were interpolated onto 0.01

x 0.01 grid. Following the same method as presented in Jiang et al., (2008b), flux F_i at each pixel was calculated:

$$S_i = \frac{\Delta Lon}{2\pi} \cdot 2 \cdot \pi \cdot R^2 \cdot [\sin(Lat_i + \frac{1}{2}\Delta Lat) - \sin(Lat_i - \frac{1}{2}\Delta Lat)] \quad (4)$$

where S_i is the total area surrounding pixel i; ΔLon and ΔLat are the longitude and latitude intervals of the grid respectively, Lat_i is the latitude at pixel i, and R is the radius of the earth. The area-averaged CO_2 flux was calculated as followed (Jiang et al., 2008b):

$$F_{\text{area-averaged}} = \frac{1}{S_1 + S_2 + \dots S_n} \cdot \sum_{i=1}^{n} F_i \cdot S_i \quad (5)$$

Because there is no precise method to account for the uncertainties of air-water CO_2 fluxes, we followed the same approach as described in Jiang et al., (2008b). Atmospheric measurements for each cruise and gas transfer velocities of Wanninkhof et al., (2009) and Wanninkhof (2014) were used to estimate standard deviations of the atmospheric CO_2 and CO_2 flux, respectively.

2.3 Temperature-normalized pCO_2 estimation

Temperature changes are important as they influence surface water pCO_2 by governing the thermodynamic equilibrium of the inorganic carbon system (Takahashi et al., 1993). If only controlled by temperature change and no other physical (mixing) or biogeochemical changes, pCO_2 in surface seawater would double for every 16°C increase ($\partial \ln pCO_2/\partial T$ = 0.0423°C) (Takahashi et al., 1993). The temperature constant above determined by Takahashi et al., (1993) works well for open ocean waters with salinities between 34 and 36 as physical mixing with freshwater is generally minor. After temperature normalization, one may attribute the remaining pCO_2 change to non-thermal processes (mostly biological activity but possibly also mixing processes). However, in coastal oceans mixing is often serious and influences the interpretations of observed temperature dependences. For example, Jiang et al., (2008a) found that values of $(\partial \ln pCO_2/\partial T)/pCO_2$ in river- and marine-dominated estuaries were less (about 0.027-0.042ºC^{-1}) than that determined by Takahashi et al., (1993). We suggest that a thermodynamic prediction for estuarine water should be used for such comparisons (Bai et al., 2015). We first derived temperature constants for a general estuarine system using the Excel macro CO2SYS (Pierrot, 2006) and inorganic carbon dissociation constants from Millero et al., (2006) for estuarine waters (S < 30) and from Mehrbach et al., (1973) refit by Dickson and Millero (1987) for high salinity

waters (S > 30). Based on data collected over the past two years, river and ocean end-members of TA (900 and 2300 μmol kg^{-1}, respectively) and of DIC (960 and 2000 μmol kg^{-1}, respectively) were used. Calculated pCO_2 varied among different temperatures, from 5 to 30ºC, with the largest difference in low salinities (0 to 5) (Fig. 2). In turn, when binning salinities to intervals of 5 units, the greatest variability in temperature constants was observed in salinities 0-5 and 5-10 (Table 1). Averaged values of $(\partial \ln pCO_2/\partial T)/pCO_2$ for salinity intervals between 0-35 ranged from 0.0332 to 0.0420 $^oC^{-1}$ (Table 1). Similar to the results found in Jiang et al., (2008a), temperature derived constants were lower than the isochemical seawater constant 0.0423$^oC^{-1}$ determined by Takahashi et al., (1993). Thus, knowing the extensively complex nature of estuarine systems, it is important to note that derived variances in temperature-normalized pCO_2 provide only a relatively simple analysis of seasonal pCO_2 fluctuations due to temperature and biological processes as it neglects the impact that various physical processes, turbulent forces, and tidal mixing scenarios have on pCO_2 dynamics.

Using a similar approach as in Takahashi et al., (2002), we also attempted to separate the temperature effect from other non-thermal effects on seasonal pCO_2 change. We first normalized the pCO_2 at in-situ temperature to the 10-year (2004-2014) annual mean temperature of 13.3ºC via the following (Takahashi et al., 2002):

$$(pCO_{2obs} \text{ at } T_{mean}) = (pCO_2)_{obs} \cdot \exp[C_s(T_{mean} - T_{obs})] \quad (6)$$

where T is temperature (°C), C_s is the averaged $(\partial \ln pCO_2/\partial T)/pCO_2$ value for the salinity interval, and subscripts "mean" and "observed" indicate the annual mean and observed values, respectively. Through this approach, we attributed any differences between calculated and observed pCO_2 values to be the result of biological activity and/or physical mixing processes (non-thermal). Because salinity gradients down the estuary vary greatly depending on the season, river discharge, tidal cycle, precipitation, and other circulation processes, salinity-binned climatologies can provide crucial insight and a different perspective to the various physical and biological controls behind observed pCO_2 distributions that geographic boundaries may not. In turn, pCO_2 values from each survey were constructed into salinity-binned climatologies (intervals of five units from 0-30) to better isolate and interpret the thermal versus non-thermal effects on seasonal pCO_2 fluctuations. Observed pCO_2 values during months with no surveys were estimated by linearly regressing data from adjacent months with sample measurements. In contrast, to best analyze the effect of temperature changes on observed pCO_2 values, annual

mean pCO_2 values across each salinity interval were used in conjunction with the mean and observed temperatures via the following equation (Takahashi et al., 2002):

$$(pCO_{2mean} \text{ at } T_{obs}) = (pCO_2)_{mean} \cdot \exp[C_s(T_{obs} - T_{mean})] \quad (7)$$

Using this method, we attributed any differences between calculated mean versus observed pCO_2 values as a result of seasonal temperature changes. To remove the temperature effect from observed in situ pCO_2, the observed pCO_2 values were normalized to a constant temperature of 13.3ºC, which was the 10-year annual mean water temperature measured in the Delaware Estuary from 2004 to 2014.

2.4 Estuarine and river CO_2 contributions

Due to various CO_2 sources such as the degradation of organic matter, discharge of sewage effluents, soil induced respiration, freshwater runoff, and addition of humic substances, river water flowing into estuarine systems are typically supersaturated in CO_2 with respect to the atmosphere (Raymond et al., 2000; Abril and Borges, 2004; Borges et al., 2006). To investigate the influence of river-borne CO_2 input to overall air-water CO_2 fluxes, we used similar methods as performed in Jiang et al., (2008a). In situ DIC and TA measurements were coupled using the Excel macro CO2SYS (Pierrot, 2006) and inorganic carbon dissociation constants from Millero et al. (2006) for estuarine waters to calculate dissolved CO_2 concentrations. We first estimated the contribution of the ocean end-member to the estuarine DIC alone as follows (Jiang et al., 2008a):

$$DIC_{mixing\ w/o} = \frac{S_i}{S_{ocean}} \cdot DIC_{ocean} \quad (8)$$

where $DIC_{mixing\ w/o}$ is the DIC concentration after the ocean end-member is diluted by fresh water with zero DIC and S_i and S_{ocean} are in situ and ocean end-member salinities, respectively (Fig. 3A). When DIC inputs from both the river and the ocean end-members were considered, estuarine DIC was estimated using a two end member mixing model as follows (Jiang et al., 2008a):

$$DIC_{mixing\ w/R} = \frac{S_i}{S_{ocean}} \cdot DIC_{ocean} + \left(1 - \frac{S_i}{S_{ocean}}\right) \cdot DIC_{river} \quad (9)$$

where $DIC_{mixing\ w/R}$ is the DIC concentration after mixing of river and ocean end-members and DIC_{river} is the river end-member (Fig. 3A). With much of the DIC pool dominated by carbonate and bicarbonate ions, Sharp et al., (2009) observed small seasonal influences on DIC concentrations due to temperature affects and biological activity. They suggest that the majority

of variability in DIC in the upper tidal river of the Delaware Estuary is due to the combined interaction of varying precipitation rates and prior meteorological conditions. This is expected as river DIC and TA are largely a dilution of weathering production by rain (Cai et al., 2008). However, at higher salinities, any drawdown of DIC relative to salinity is small since less than 1% of the DIC pool exists as pCO_2 (Sharp et al., 2009). Thus, while total DIC concentrations illustrate some fluctuations in biological activity (which occurred mostly at the highly productive mid-bay), it is an integrated measurement of freshwater and seawater mixing (Sharp et al., 2009). $TA_{mixing\ w/o}$ and $TA_{mixing\ w/R}$ were also estimated using similar equations by replacing DIC with TA (Fig. 3B). Because CO_2 concentrations do not change linearly during mixing, they were estimated using corresponding DIC and TA mixing values (Fig. 3C) (Jiang et al., 2008a). Moreover, since CO_2 concentrations fluctuate with temperature change, the 10-year (2004-2014) annual mean temperature of 13.3 ºC was used in this work. Thus, the CO_2 contribution due to river input ($\Delta[CO_2]_{riv}$) was estimated as follows:

$$[CO_2]_{riv} = [CO_2]_{mixing\ w/R} - [CO_2]_{mixing\ w/o} \quad (10)$$

Calculated river CO_2 inputs ($[CO_2]_{riv}$) and combined river discharges from the Schuylkill and Delaware Rivers for each month were used to compute river-borne CO_2 fluxes in the upper tidal river.

To further investigate the influence of CO_2 inputs from the river (external) versus production from within the estuary (internal), we used a similar but modified method as performed in Jiang et al., (2008a). The CO_2 contribution from within the estuarine zone ($[CO_2]_{est}$) was estimated as follows:

$$[CO_2]_{est} = [CO_2]_i - [CO_2]_{mixing\ w/R} + (\tau_i \cdot F_i) \quad (11)$$

where ($[CO_2]_i$) is the in situ CO_2 concentration, τ_i is the flushing time, and F_i is the air-water CO_2 flux. Specifically, ($[CO_2]_i$) was calculated using in situ DIC and TA concentrations and τ_i was estimated using river discharge rates and volume of each region (Table 3) (Sheldon and Alber, 2002). Surveys that did not contain sufficient river end-member DIC and TA measurements were excluded. Alternatively, Eq. (11) suggests that integrated CO_2 degassing ($\tau_i \cdot F_i$) is supported by the deficit or excess CO_2 concentration ($[CO_2]_{mixing\ w/R} - [CO_2]_i$) plus the internal estuarine CO_2 production or consumption ($[CO_2]_{est}$) exhibited across each region.

3 Results

3.1 Hydrographic conditions

Measured surface water temperatures and river discharge during each cruise were compared with the 10-year (2004-2014) and 30-year (1980-2014) monthly averages for surface water temperatures and Delaware River discharge rates, respectively. Water temperatures were slightly cooler than the 10-year average during March 2014, June 2013, and July 2014, while water temperatures during the rest of the cruises were slightly warmer (Fig. 4A) (USGS gauge 01463500). Discharge conditions during each survey were compared with the 30-year average discharges from 1980 to 2014 (Fig. 4B) (USGS gauge 01463500). The Delaware River discharge was greatest during March 2014 and June 2013. Discharges were smallest during August 2014, October 2013, November 2013, and November 2014. Of the four low-flow months, all of them except for August 2014 had discharge rates less than one standard deviation of the 30-year average.

The surface water salinity distributions confirm the various river discharge conditions recorded throughout each survey (Fig. 5A-I). Salinity < 1.0 was reached on six of the nine cruises (Fig. 5A, 5B, 5C, 5E, 5G, and 5H). The July 2014, August 2013 and October 2013 cruises only transected as far north as the Chesapeake-Delaware Canal (about 39.55ºN) (Fig. 1). Salinity < 1.0 (a minimum of 0.98) was only observed during the July 2014 excursion, which had the highest river discharge of the three partial surveys (Fig. 5C). Generally, high salinity waters (25-32.5) were observed in the lower bay and salinities around 20 to 25 in the mid-bay. The upper bay had a much broader scale ranging from salinities 10 to 20 and during the high flow months of March 2014 and June 2013 salinities < 10 were observed (Fig. 5A and 5B). Salinities did not reach less than 0.25 in the turbidity maximum zone. Salinity distributions in the urban river were limited due to the lack of surveys conducted in this region.

3.2 Surface water pCO_2

Generally, surface water pCO_2 in the Delaware Estuary increased from the ocean to the river end-member with pCO_2 values ranging from about 150 to over 4000 µatm (Fig. 6A-I). Moreover, pCO_2 exhibited strong seasonal variations across both river and bay portions. The most pronounced shifts in surface water pCO_2 were observed within the lower urban river and turbidity maximum river zones of the Delaware River with pCO_2 being lowest in the cool months (March, October, and November) and highest in the warm months (June, July, and August) (Table 2). During all months, the turbidity maximum zone was supersaturated in CO_2

with respect to the atmosphere (atmospheric pCO_2: 375-398 µatm) except during March 2014 (Fig. 6A). Throughout the summer and early fall (June, July, and August), pCO_2 ranged from about 650 µatm to over 4000 µatm across the turbidity and lower urban river zones (Fig. 6B-E). In late fall (October and November), pCO_2 dropped to as low as 500 µatm in the turbidity maximum zone and reached 1400 µatm within the lower urban river zone (Fig. 6F-H). However, the decrease in pCO_2 values were not always observed as temperatures cooled. During the winter (December), surface water pCO_2 values increased across the turbidity maximum zone ranging from about 650 to 1000 µatm (Fig. 6I). As discussed later, this shift in pCO_2 during winter is likely a result of opposing timing of seasonal temperature cycles and respiration versus that of river discharge rates.

Surface water pCO_2 exhibited strong seasonal variations in the Delaware Bay as well (Fig. 6A-I). In March 2014, most likely due to a strong biological bloom and low temperature (Fig. 4A), the entire bay system (upper, mid-, and lower) was under-saturated in CO_2 with respect to the atmosphere (Table 2). In particular, pCO_2 reached as low as 160 µatm in the mid-bay (Fig. 6A). During the warmer summer months (June, July, and August), pCO_2 in the bay remained around 400 to 500 µatm with occasional undersaturation occurring in the mid-bay region (Fig. 6B-E). In August 2014, low pCO_2 ranging from about 200 to 350 µatm was observed throughout much of the mid- and lower bay regions (Fig. 6E). In contrast, during the late fall pCO_2 values were fairly homogenous throughout the mid- and lower bay (400-450 µatm in October 2013 and 2014 and 375-415 µatm in November 2013) and slightly higher pCO_2 occurring in the upper bay (Fig. 6F-H). In December 2014, pCO_2 increased throughout all regions of the bay with pCO_2 values ranging from 500 to 650 µatm (Fig. 6I). While reasons to support the elevated pCO_2 values remain unclear, stratification of subsurface waters in late fall followed by strong winter mixing during winter (December 2014) and a two-fold increase in river discharge could explain the elevated pCO_2 values observed throughout the mid- and the lower bay systems (Fig. 4B).

3.3 Air-water CO_2 fluxes

The urban river and turbidity maximum zone served as strong sources of CO_2 to the atmosphere and was positive during all months (Table 2). Across the upper to lower bay portions of the estuary, uptake of CO_2 from the atmosphere was greatest during spring (March) ranging from F_{CO2} = -12.1 to -20.0 mmol m^{-2} d^{-1} (Table 2). The CO_2 uptake flux was highest in March 2014 in the mid-bay (-20.0 mmol m^{-2} d^{-1}), while the highest CO_2 degassing flux occurred in June 2014 in

the urban river (144.8 mmol m^{-2} d^{-1}) (Table 2). Air-water CO_2 fluxes in the upper to lower bay regions decreased in early winter (December) to a minimum in early spring (March), followed by an increase to an annual maximum in early summer (June). In the turbidity maximum zone and urban river, area-averaged CO_2 fluxes followed the same seasonal decrease in spring and increase in summer but reached an annual minimum in late fall instead of early spring. In winter (December), the mid- and lower bays, which were typically sinks or weak sources of CO_2, exhibited relatively strong CO_2 fluxes to the atmosphere.

3.4 CO_2 distribution across the salinity gradient

To further investigate pCO_2 variations along the Delaware Estuary, we examined distributions of pCO_2 across the salinity gradient. Due to limited area and salinity coverage, surveys conducted in August and October 2013 were excluded for this assessment. In all months, pCO_2 versus salinity followed a concave upward trend towards the river end-member (Fig. 7). The seasonal variation between pCO_2 values was largest at low salinities around 0 to 5 with pCO_2 values in the summer (June, July, and August) nearly two-fold greater than those observed in the spring (March) and fall (October and November) seasons (Fig. 7). In all seasons, pCO_2 was supersaturated with respect to the atmosphere from salinities 0 to 5. In spring, undersaturated pCO_2 was observed over the widest salinity range from 7.5 to 30. In summer, undersaturated pCO_2 was generally not observed except at moderate salinities around 17 to 28 in August. In fall, pCO_2 values were near atmospheric concentrations around mid-salinity waters and were only undersaturated at salinities greater than 25. In winter (December), pCO_2 values were always supersaturated with respect to the atmosphere across the entire salinity range. Seasonally, the Delaware Estuary served as a strong CO_2 sink (-5.0 ± 6.0 mol-C m^{-2} yr^{-1}) in the spring, a strong source (4.9 ± 8.1 mol-C m^{-2} yr^{-1}) in the summer, a weak source (1.0 ± 2.4 mol-C m^{-2} yr^{-1}) in the fall, and a strong source (5.7 ± 1.9 mol-C m^{-2} yr^{-1}) in the winter. While low salinity waters were strong CO_2 sources, proportionally these upper regions ($0 \leq S < 10$) were small in comparison to the total estuarine study area. In turn, their area-averaged contribution (27.1 ± 6.4 mol-C m^{-2} yr^{-1}) to overall regional flux (2.4 ± 4.8 mol-C m^{-2} yr^{-1}) is minor. Thus, the Delaware Estuary as a whole acts as a relatively weak CO_2 source (2.4 ± 4.8 mol-C m^{-2} yr^{-1}), which is in great contrast to many river estuaries that are strong CO_2 sources (26 ± 21 mol-C m^{-2} yr^{-1}) (Borges and Abril, 2011).

3.5 Seasonal variations in temperature-normalized pCO_2

Seasonal distributions of pCO_{2obs} at 13.3 ºC, which indicate impacts of non-thermal processes (biological and mixing), varied noticeably throughout the year and across salinity intervals (Fig. 8). Typically, pCO_{2obs} at 13.3 ºC was greatest during early and mid-winter season (December and January) except in the 0-5 salinity interval (mostly turbidity maximum zone and urban river) when pCO_{2obs} at 13.3 ºC reached its maximum in June. Coupled with decreasing flow, in the 0-5 salinity interval, pCO_{2obs} at 13.3 ºC decreased from June to an annual minimum in October. In the mid- salinity waters ($5 \leq S \leq 20$), pCO_{2obs} at 13.3 ºC decreased from mid-winter to an annual minimum in March, followed by an increase to a secondary maximum in June. In contrast, in the high salinity waters ($20 \leq S \leq 30$) of the lower bay where biological removal of CO_2 was generally strong, annual minimums were observed in August. The annual distribution of pCO_{2mean} at T_{obs}, which indicates the impact of the seasonal thermal cycle, followed typical bell shaped curves across all salinity intervals with the lowest values occurring in winter and an annual maximum occurring in July.

4 Discussion

The seasonal and spatial distributions of estuarine pCO_2 is governed by the dynamic interaction between water temperature, horizontal and vertical mixing processes, biological processes, and CO_2 contributions from the river, ocean, and estuarine zone (Jiang et al., 2008a; Borges and Abril, 2011; Hunt et al., 2014). In the estuarine zone, the addition or removal of CO_2 include net ecosystem metabolism, DIC exchange with intertidal marshes, sediments, groundwater inputs, air-water gas exchanges, and other estuarine contributing processes (Jiang et al., 2008a). In the following sections, we evaluate the impact that seasonal temperature changes and river discharge rates have on surface water pCO_2 distributions, river and estuarine CO_2 inputs, and river-borne CO_2 fluxes throughout the Delaware Estuary.

4.1 Temperature vs. biological effects on pCO_2

Similar to other estuaries (Borges and Abril, 2011), seasonal temperature changes provided a first control on the observed seasonal changes in pCO_{2obs} (low in the winter and high in the summer, Fig. 4A and 7). This is further reflected in the fact that temperature-normalized pCO_2 was always higher than in situ pCO_2 in the winter but lower than in situ pCO_2 in the summer (Fig. 8). Presumably, then, seasonal patterns of the temperature-normalized pCO_2 reflect how non-thermal processes (mixing and biological) influence in situ pCO_2. For example, in the urban

river and turbidity maximum zones (S < 5), high pCO_{2obs} at 13.3 ºC in the spring and winter may reflect both river inputs and strong respiratory CO_2 production. Low pCO_{2obs} at 13.3 ºC during the warmer months likely reflect the removal of CO_2 due to various non-thermal processes. During the warmer months from May to October, Yoshiyama and Sharp (2006) found elevated nitrite (NO_2) concentrations in the urban river when nitrification and primary production were highest. In addition, high NO_2 concentrations were observed in the mid-bay in summer when primary production was maximal (Pennock and Sharp, 1994). Comparably, pCO_{2mean} at T_{obs} (changes due to the seasonal thermal cycle) trends were opposite to that of pCO_{2obs} at 13.3 ºC with lower than pCO_{2obs} values in the winter and higher than pCO_{2obs} values in the summer. These opposing signals suggest that increases in surface water pCO_2 due to winter-to-summer warming are partially compensated by the reduction of surface water pCO_2 due to mixing processes and/or biological removal of CO_2 (Takahashi et al., 2002). Sharp et al. (2009) found that during the March-April period ammonium (NH_4), phosphate (PO_4), and silicate (Si) concentrations were heavily depleted in the mid- and lower bay regions due to extensive spring blooms. Similarly, but in the opposite direction, the reduction in surface water pCO_2 due to fall-to-winter cooling is partially compensated by the elevation of surface water pCO_2 caused by various non-thermal processes (Fig. 8).

We further examine the relative importance of the temperature and biological effects in each salinity interval by calculating the ratio of ΔpCO_{2temp} to ΔpCO_{2bio} (T/B). Using similar methods as performed in Takahashi et al., (2002), we calculate the thermal effects on surface water pCO_2 in each salinity interval as follows:

$$\Delta pCO_{2thermal} = (pCO_{2mean} \text{ at } T_{obs})_{max} - (pCO_{2mean} \text{ at } T_{obs})_{min} \quad (12)$$

where $(pCO_{2mean} \text{ at } T_{obs})_{max}$ and $(pCO_{2mean} \text{ at } T_{obs})_{min}$ are the maximum and minimum pCO_{2mean} at T_{obs} values, respectively. In other words, the thermal effects on the mean annual pCO_2 value is represented by the seasonal amplitude of (pCO_{2mean} at T_{obs}) values computed using Eq. (7). Likewise, the non-thermal effects (biological and mixing processes) on surface water pCO_2 were calculated as follows (Takahashi et al., 2002):

$$\Delta pCO_{2non\text{-}thermal} = (pCO_{2obs} \text{ at } 13.3\ ^oC)_{max} - (pCO_{2obs} \text{ at } 13.3\ ^oC)_{min} \quad (13)$$

where $(pCO_{2obs} \text{ at } 13.3\ ^oC)_{max}$ and $(pCO_{2obs} \text{ at } 13.3\ ^oC)_{min}$ are the maximum and minimum pCO_{2obs} at 13.3 ºC values, respectively. Thus, the non-thermal thermal effects on surface water pCO_2 (pCO_{2obs} at 13.3 ºC) is represented by the seasonal amplitude of pCO_2 values corrected to

the 10-year (2004-2014) annual mean temperature using Eq. (6). The relative importance of these effects in each salinity interval can be expressed as the difference between $\Delta pCO_{2thermal}$ and $\Delta pCO_{2non\text{-}thermal}$ ($T - B$) or the ratio of $\Delta pCO_{2thermal}$ to $\Delta pCO_{2non\text{-}thermal}$ (T/B). In estuarine regions where thermal effects on surface water pCO_2 exceed non-thermal effects, the (T/B) ratio is greater than 1 or ($T - B$) is positive, whereas in areas where non-thermal effects dominate, the (T/B) ratio is less than 1 or ($T - B$) is negative. Based on our results, temperature was a dominant factor in controlling surface water pCO_2 in low salinity waters ($0 \leq S \leq 10$) (mainly the urban river and turbidity maximum zone) with T/B ratios ranging from 1.30 to 1.68 (Table 4). As salinity increased, both $\Delta pCO_{2thermal}$ and $\Delta pCO_{2non\text{-}thermal}$ decreased (Table 4). The decrease in $\Delta pCO_{2thermal}$ may be attributed to the reduction in river water temperatures at the ocean end-member (Hunt et al., 2014). In comparison to the upper tidal river, low T/B ratios ranging from 0.69 to 0.80 were observed in mid-salinity waters ($15 \leq S \leq 25$) (mainly the mid- and lower bay) suggesting that pCO_2 distributions in the Delaware Bay are largely governed by biological and/or mixing processes.

4.2 Influence of river-borne CO_2 on estuarine degassing

The potential emission of river-borne CO_2 was estimated based on the concept of excess CO_2, the difference between the in-situ DIC at zero salinity and a theoretical DIC value at atmospheric equilibrium (ΔDIC) (Abril et al., 2000; Borges et al., 2006). The theoretical DIC was computed using in-situ TA values and an atmospheric pCO_2 of 395 µatm. River-borne CO_2 fluxes were calculated as the product of ΔDIC and the combined river discharges from the Schuylkill and Delaware Rivers for each month divided by the estuarine surface area. Generally, as freshwater residence time increases (river discharge decreases) river-borne CO_2 fluxes decrease (Borges et al., 2006). As more river-borne CO_2 is released into the atmosphere in the upper estuary due to increased residence time, leaving less river-borne CO_2 for degassing in the lower estuary, the overall contribution of CO_2 emissions are largely shaped by the net community production in the mixed layer (ML NCP) in the mid- to high salinity estuarine zones (Abril et al., 2000; Borges et al., 2006). In comparison, as freshwater residence time decreases (river discharge increases), DIC enrichment from ML NCP is reduced and river-borne CO_2 fluxes increase. In certain cases, such as the Rhine estuary or other systems with extremely rapid flushing times, residence time is so short that not all of the river-borne CO_2 is ventilated to the atmosphere in the estuarine zone (Borges and Frankignoulle, 2002; Borges et al., 2006). In turn, the potential emission of river-

borne CO_2 is higher than the actual observed air-water CO_2 fluxes from the estuary (Borges et al., 2006).

Positive correlations between river-borne and air-water CO_2 fluxes illustrate the importance of river inputs to CO_2 degassing fluxes (Fig. 9). In the Delaware Estuary, the largest river-borne CO_2 flux was observed during the highest flow month of June 2013 with river CO_2 flux accounting for 119% and 60% of the overall CO_2 degassing flux in the urban river and turbidity maximum zone, respectively (Fig. 9). Moreover, during the high flow month of March 2014, river-borne CO_2 fluxes exceeded 200% and 150% of the overall CO_2 degassing fluxes in the urban river and turbidity maximum zone, respectively (Fig. 9). Presumably, the higher river-borne to overall CO_2 fluxes in March are due to the combined influence of increased river discharge coupled with large CO_2 consumption in the estuary (Fig. 4B and 5A). This is consistent with the observed low pCO_2 and high O_2 values (Fig. 6A) (Cai unpublished data). In contrast, in July and August 2014, air-water CO_2 fluxes exceeded river-borne CO_2 fluxes indicating strong estuarine CO_2 production. Such internal estuarine CO_2 production is most likely due to respiration in the water column, but may also include other inputs such as benthic respiration and net respiration from surrounding intertidal marshes. In turn, while correlations between river-borne and air-water CO_2 fluxes were exhibited, differences between the two fluxes suggest that the input of CO_2 from other estuarine sources is important.

4.3 Internal estuarine production versus river CO_2 input

Our results illustrate that both the river and the estuarine zone contribute to CO_2 inputs in the Delaware Estuary (Fig. 10). Combined river CO_2 input and internal estuarine production were highest in the urban river (87.8 to 255.4 μmol L^{-1}) and smallest in the lower bay (-38.8 to 7.0 μmol L^{-1}) (Fig. 10). In the tidal river, internal estuarine production exhibited clear seasonal trends with CO_2 contributions being lowest in the spring (March), highest in the summer (June and August), and medium in the fall (October and November). Strong seasonal trends in internal estuarine production were also observed in the bay regions. During spring and late summer (March and August 2014), internal estuarine CO_2 signals were negative in the mid- and lower bay zones and reached as much as eight folds greater than total river CO_2 inputs, ranging from -22.9 to -100.4 μmol L^{-1} (Fig. 10). Thus, the majority of river CO_2 input was heavily compensated by the biological removal of CO_2 in the bay waters. In addition, during spring season (March) high CO_2 consumption was also observed in the upper bay with internal estuarine CO_2 signals (-

30.7 µmol L-1) exceeding total river CO_2 contribution (25.7 µmol L^{-1}) (Fig. 10). Depending on river discharge rates, the freshwater residence time in the Delaware Estuary ranges from about 40-90 days (Ketchum, 1952). Due to smaller physical sizes, freshwater residence time in the upper tidal river is much shorter (Table 3). Thus, the percentage of river-borne CO_2 in the upper Delaware Estuary is large (Fig. 10), and that percentage decreases in the mid- and lower bays, which have longer residence times and high biological CO_2 removal (Sharp, 1983).

4.4 Assumptions and limitations

While this study serves as the first air-water CO_2 flux product in the Delaware Estuary, there are several limitations. First, the lack of cross-bay transects (east to west), except in December 2014, limits our knowledge of surface water pCO_2 distributions in shallow waters regions of the bay system. Due to various biological and physical processes (i.e. influence from nearby tidal marshes, tributaries, or estuarine circulation forces), surface water pCO_2 may vary from within the main channel to the perimeters of the estuary. Jiang et al., (2008a) found that surface water pCO_2 and air-water CO_2 flux in the marine-dominated Sapelo and Doboy sounds paralleled seasonal temperature changes and net CO_2 inputs from within the estuarine zone. Due to intense productivity of vegetation in the surrounding salt marshes, extensive accumulation of organic carbon occurs during spring and early summer (Dai and Wiegert, 1996; Jiang et al., 2008a). During late summer and early fall, increased surface water temperatures coupled with tidal flushing of intertidal marsh waters and the decomposition of dead plants contribute to high CO_2 degassing in these estuaries (Dai and Wiegert, 1996; Cai and Wang, 1998; Cai et al., 1999; Neubauer and Anderson, 2003; Wang and Cai, 2004). However, due to the much broader geographic size of the Delaware Bay compared to the marine-dominated Sapelo and Doboy sounds, in-water biological processes are most likely important. In turn, the impact from the growth and decay of marsh plants on surface water pCO_2 and CO_2 flux dynamics may not be as influential in the Delaware Bay except near the shorelines where tides regularly flush marsh boundaries. Studies conducted by Culberson et al., (1987) and Lebo et al., (1990) performed several cross bay transects sampled at various depths, over diel cycles, within tributaries, and periodically offshore. Results showed that cross-bay gradients were inconsistent and relatively small, except in shallow waters near the shoreline where total suspended sediment and chlorophyll concentrations were frequently elevated (Culberson et al., 1987; Lebo et al., 1990; Sharp et al., 2009). Thus, the impact from marsh input of DIC to the Delaware Bay on overall

pCO_2 distributions and associated CO_2 degassing fluxes are most likely small. During December 2014, pCO_2 measurements were not only collected in the main channel, but also near the Delaware and New Jersey perimeters of the bay (Fig. 6I). While slight variability was observed across the bay, pCO_2 values from the lower to upper bay regions remained within about 150 µatm (Fig. 6I and Table 2).

In addition to the lack of cross bay transects, there is a pressing need to conduct more winter and early spring surveys to fully cover seasonal ranges in key properties such as temperature and river discharge rates. Moreover, cruises or moored sensor studies at or around large discharge events are needed. Recent study by Voynova and Sharp (2012) found that in the past century there have been a recorded 54 extreme discharges (defined by the average daily discharge as recorded in Trenton, NJ from 1 Oct 1912 to 30 Sept 2011 plus 10 standard deviations); 46% of these occurring in the past decade (Voynova and Sharp, 2012). With increasing evidence suggesting that extreme weather events will occur more frequently with climate change, it is important to maintain routine seasonal surveys to learn how such subsequent conditions (i.e. increased summer stratification, riverine CO_2 fluxes, removal of oxygen in bottom waters) impact various coastal environments (Allan and Soden, 2008; Yoana and Sharp, 2012). Furthermore, more research is needed in the urban and upper river sections of the estuary to better understand CO_2 dynamics throughout the whole estuarine gradient. The lack of inorganic carbon data in these upper regions limits syntheses of regional CO_2 fluxes and generalizations to underlying mechanisms. Routine sampling along small tributaries and river systems could provide crucial insight to the biogeochemistry in the upper tidal river.

There are also several limitations to the temperature-normalized and end-member mixing models that need to be addressed. First, knowing the extensively complex nature of estuarine systems, it is important to note that derived variances in temperature-normalized pCO_2 provide only a relatively simple analysis of seasonal pCO_2 fluctuations due to thermal and non-thermal processes as it neglects the impact that various physical processes, turbulent forces, and tidal mixing scenarios have on pCO_2 dynamics. However, as mentioned before, since salinity fluctuates greatly depending on factors such as season, river discharge, and tidal cycle, salinity-binned climatologies can provide crucial insight to various physical and biological controlling mechanisms behind pCO_2 distributions that geographic boundaries may not. Unfortunately, due to the lack of winter surveys and unusually high pCO_2 values in December, interpolated

temperature-normalized pCO_2 during cooler months may be biased and slightly overestimated. Moreover, the temperature derived constants ($\partial \ln pCO_2/\partial T$) derived in this study were based on river and ocean end-member TA and DIC concentrations collected in the Delaware Estuary over the past two years. Thus, it is important to note that derived temperature constants here are applicable for general estuarine systems and may not be suitable for coastal environments with different hydrological and/or geochemical characteristics.

In situ DIC and TA measurements were coupled using the Excel macro CO2SYS (Pierrot, 2006) and inorganic carbon dissociation constants from Millero et al. (2006) for estuarine waters to calculate dissolved CO_2 concentrations. While river and ocean end-members were obtained at near zero salinity and at the mouth of the bay, respectively, no fixed end-member sampling locations were established. This marginal difference in end-member location could slightly increase or decrease estimated CO_2 concentrations. In the chemical model of the CO2SYS, NH_3, NH_4^+, and organic matter contribution to TA were not included (Cai et al., 1998; Cai et al., 2010b), which were likely high in low salinity waters. Thus, lower calculated CO_2 than observed CO_2 was expected as the observed TA included other acid-base components (Fig. 3C). However, due to the very high pCO_2, such uncertainty is deemed unimportant in our consideration. Another factor that may contribute to the lower calculated CO_2 than observed CO_2 could be the use of mercuric chloride as a preservative in low salinity samples ($S < 10$) (Trabalka and Reichle, 2013). Excess alkalinity generated via the dilution of mercuric chloride could contribute to conservative CO_2 flux estimates (Trabalka and Reichle, 2013) although due to the relatively high TA in the Delaware River we believe this effect is small.

5 Summary and concluding remarks

While the urban river and turbidity maximum zone are strong CO_2 sources to the atmosphere, these upper regions are small in comparison to the bay regions of the Delaware Estuary. Thus, overall the Delaware Estuary acts as a relatively weak CO_2 source (2.4 ± 4.8 mol-C m^{-2} yr^{-1}) in comparison to many other estuarine systems that serve as strong CO_2 sources to the atmosphere (26 ± 21 mol-C m^{-2} yr^{-1}) (Borges and Abril, 2011). Of the 62 estuaries compiled in Borges and Abril (2011), only the Aby Lagoon, a permanently stratified system, served as a sink for atmospheric CO_2. Seasonal temperature cycles influence the rise and fall of surface water pCO_2 throughout the Delaware Estuary, but these effects are partially compensated by opposing cycles

of biological removal and addition of CO_2. Moreover, positive correlations between river-borne degassing to overall CO_2 fluxes in the upper sub-sections of the estuary (the urban river and turbidity maximum zone). Such features are typical for rapidly flushing river-dominated estuaries. While river-borne CO_2 degassing fluxes heavily impact CO_2 dynamics throughout the upper Delaware Estuary, these forces are largely compensated by internal biological processes within the extensive bay system of the lower estuary.

Along the eastern Georgia (USA) coast, Jiang et al., (2008a) identified the Altamaha Sound as a river-dominated estuary with CO_2 fluxes driven by river discharge. Comparably, the Kennebec estuary, located on the central Maine (USA) coast, exhibited high river CO_2 inputs and short freshwater residence times (~ 4 days) suggesting that CO_2 sources in the estuary were mainly controlled by the degassing of river-borne DIC (Hunt et al., 2014). The upper Delaware Estuary showed similar results with high river CO_2 contributions and rapid freshwater transit times during all months (Fig. 10 and Table 3). In contrast, in systems with long freshwater residence times (i.e. the Delaware Bay and Scheldt estuary), much, if not all, of the river-borne CO_2 is released into the atmosphere (Abril et al., 2000; Borges et al., 2006). In turn, overall CO_2 emission from the estuary is largely controlled by net community production in the mixed layer (ML NCP) (Borges et al., 2006). In the case of the European Scheldt estuary, long freshwater residence time (30 - 90 days) leads to extensive DIC enrichment in the water column and high CO_2 emissions to the atmosphere (Abril et al., 2000; Borges et al., 2006). Similarly, and in contrast to the rapidly flushing Altamaha Sound, Jiang et al., (2008a) identified the marsh surrounded Sapelo Sound as a marine-dominated estuary with CO_2 fluxes driven by seasonal temperature and metabolic cycles.

With its extensive geographic size, the Delaware Estuary features both a river-dominated upper estuary and an ocean-dominated lower bay. In this case, air-water CO_2 fluxes in the heterotrophic upper estuary are significantly influenced by intense river-borne CO_2 degassing akin to the river-dominated Altamaha Sound and Kennebec estuary. The autotrophic lower estuary is governed by water-column biological processes and seasonal temperature cycles akin to the marine-dominated Sapelo Sound and Scheldt estuary (though the Delaware Estuary and other large estuarine systems are on orders of magnitude more productive than smaller marine-dominated estuaries).

The continuation of research cruises on estuarine and coastal margins can provide crucial insight to the physical and biological changes in the past, present, and future ocean systems. Such extensive surveys, collection of carbonate parameters, and comparison of carbonate parameters over time, can significantly broaden our understanding of the processes that govern these coastal zones. In turn, such knowledge can be used to help predict and hopefully regulate the rise of current and future threats to our coastal ocean systems.

Acknowledgements

We thank the captains and crew of *R/V Hugh R. Sharp* and *R/V Joanne Daiber* for their support. We appreciate D.L. Kirchman for his supportive comments and discussion. We thank J. H. Sharp, D. L. Kirchman, G. W. Luther III, J. H. Cohen, and B. J. Campbell for sharing their research cruises and providing us the opportunity to conduct such extensive surveys. We also thank Christopher Hunt and an anonymous reviewer for their thorough and constructive reviews. The above ships of opportunity cruises were supported by awards from the National Science Foundation (OCE-1155385, OCE-1261359, and OCE-1030306) and the Delaware Sea Grant College Program (RHCE14-DESG). Cai acknowledges UD internal funds for supporting his research.

References

Abril, G. and Borges, A.V.: Carbon dioxide and methane emissions from estuaries, in: Greenhouse gas emissions from natural environments and hydroelectric reservoirs: fluxes and processes. Environmental Science Series, edited by: Tremblay, A., Varfalvy, L., Roehm, C., and Garneau, M., Berlin, Heidelberg, New York, 187-207, 2004.

Abril, G., Etcheber, H., Borges, A. V., and Frankignoulle, M.: Excess atmospheric carbon dioxide transported by rivers into the Scheldt estuary, Cr. Acad. Sci. II A., 330, 761-768, 2000.

Abril, G., Commarieu, M. V., Sottolichio, A., Bretel, P., and Guérin, F.: Turbidity limits gas exchange in a large macrotidal estuary, Estuar. Coast. Shelf. S., 83, 342-348, 2009.

Allan, R. P. and Soden, B. J.: Atmospheric warming and the amplification of precipitation extremes, Science, 321, 1481-1484, 2008.

Bai, Y., Cai, W.-J., He, X., Zhai, W., Pan, D., Dai, M., and Yu, P.: A mechanistic semi-analytical method for remotely sensing sea surface pCO_2 in river-dominated coastal oceans: A case study from the East China Sea, J. Geophys. Res-Oceans., 120, 2331-2349, 2015.

Borges, A. V.: Do we have enough pieces of the jigsaw to integrate CO_2 fluxes in the coastal ocean? Estuaries, 28, 3-27, 2005.

Borges, A. V. and Frankignoulle, M.: Distribution of surface carbon dioxide and air-sea exchange in the upwelling system off the Galician coast, Global Biogeochem. Cy., 16, 13-1–13-13, doi:
10.1029/2000GB001385, 2002.

Borges, A. V. and Abril, G.: Carbon dioxide and methane dynamics in estuaries, in: Treatise on estuarine and coastal science, edited by: Wolanski, E. and McLusky, D., Academic Press, Waltham, 119–161, 2011

Borges, A. V., Delille, B., Schiettecatte, L.-S., Gazeau, F., Abril, G., and Frankignoulle, M.: Gas transfer velocities of CO_2 in three European estuaries (Randers Fjord, Scheldt, and Thames), Limnol. Oceanogr., 49, 1630-1641, 2004.

Borges, A. V., Delille, B., and Frankignoulle, M.: Budgeting sinks and sources of CO_2 in the coastal ocean: Diversity of ecosystems counts, Geophys. Res. Lett., 32, 1-4, 2005.

Borges, A. V., Schiettecatte, L.-S., Abril, G., Delille, B., and Gazeau, F.: Carbon dioxide in European coastal waters, Estuar. Coast. Shelf. S., 70, 375-387, 2006.

Cai, W.-J.: Estuarine and coastal ocean carbon paradox: CO_2 sinks or sites of terrestrial carbon incineration? Annu. Rev. Mar. Sci., 3, 123-145, 2011.

Cai, W.-J. and Wang, Y.: The chemistry, fluxes, and sources of carbon dioxide in the estuarine waters of the Satilla and Altamaha Rivers, Georgia, Limnol. Oceanogr., 43, 657-668, 1998.

Cai, W.-J., Wang, Y., and Hodson, R. E.: Acid-base properties of dissolved organic matter in the estuarine waters of Georgia, USA, Geochim. Cosmochim. Ac., 62, 473-483, 1998.

Cai, W.-J., Pomeroy, L., Moran, M. A., and Wang, Y.: Oxygen and carbon dioxide mass balance for the estuarine-intertidal marsh complex of five rivers in the southeastern U.S., Limnol. Oceanogr., 44, 639–649, 1999.

Cai, W.-J., Dai, M., and Wang, Y.: Air-sea exchange of carbon dioxide in ocean margins: A province-based synthesis, Geophys. Res. Lett., 33, 2-5, 2006.

Cai, W., Guo, X., Chen, A., Dai, M., Zhang, L., Zhai, W., Lohrenz, S. E., Yin, K., Harrison, P. J., and Wang, Y.: A comparative overview of weathering intensity and $HCO3^-$ flux in the world's major rivers with emphasis on the Changjiang, Huanghe, Zhujiang (Pearl) and Mississippi Rivers, Cont. Shelf. Res., 28, 1538–1549, doi:10.1016/j.csr.2007.10.014, 2008.

Cai, W.-J., Hu, X., Huang, W.-J., Jiang, L.-Q., Wang, Y., Peng, T.-H., and Zhang, X.: Alkalinity distribution in the western North Atlantic Ocean margins, J. Geophys. Res-Oceans., 115, 1-15, 2010a.

Cai, W.-J., Luther, G. W. III., Cornwell, J. C., and Giblin, A. E.: Carbon cycling and the coupling between proton and electron transfer reactions in aquatic sediments in Lake Champlain, Aquat. Geochem., 16, 421-446, 2010b.

Chen, C.-T. A. and Borges, A. V.: Reconciling opposing views on carbon cycling in the coastal ocean: Continental shelves as sinks and near-shore ecosystems as sources of atmospheric CO_2, Deep-Sea. Res. Pt. II., 56, 578–590, 2009.

Chen, C.-T. A., Huang, T. H., Chen, Y. C., Bai, Y., He, X., and Kang, Y.: Air-sea exchanges of CO_2 the world's coastal seas, Biogeosciences, 10, 6509–6544, 2013.

Cifuentes, L. A., Sharp, J. H., Fogel, M. L.: Stable carbon and nitrogen isotope biogeochemistry in the Delaware Estuary, Limnol. Oceanogr., 33, 1102-1115, 1988.

Crosswell, J. R., Wetz, M. S., Hales, B., and Paerl, H. W.: Air-water CO_2 fluxes in the microtidal Neuse River Estuary, North Carolina, J. Geophys. Res-Oceans., 117, 1–12, 2012.

Culberson, C. H.: Dissolved oxygen, inorganic carbon, and the acid–base system in the Delaware Estuary, in: Ecology and Restoration of the Delaware River Basin. Pennsylvania Academy of Science, University of Michigan, 58-76, 1988.

Culberson, C.H., Pennock, J.R., Lee, B.W., Biggs, R.B., Church, T.M., and Sharp, J.H.: Data from the YABLED cruises. September 1981- July 1984. Oceanographic data Report Number 4. Del. Sea. Grant. Program, University of Delaware, Available from Sharp, J. H., 170 pp., 1987.

Dai, T. and Wiegert, R.G.: Estimation of the primary productivity of Spartina alterniflora using a canopy model, Ecography, 19, 410-423, 1996.

Dickson, A. G. and Millero, F. J.: A comparison of the equilibrium constants for the dissociation of carbonic acid in seawater media, Deep-Sea Res., 34, 1733–1743, 1987.

Dickson, A. G., Sabine, C. L., Christian, J. R.: Guide to best practices for ocean CO_2 measurements, PICES Special Publications 3, 90-101, 2007.

Frankignoulle, M., Abril, G., Borges A.V., Bourge, I., Canon, C., Delille, B., Libert, E., and Théate, J. M.: Carbon dioxide emission from European estuaries, Science, 282, 434–436, 1998.

Gran, G.: Determination of the equivalence point in potentiometric titrations Part II, Analyst, 77, 661–671, 1952.

Huang, W.-J., Wang, Y., and Cai, W.-J.: Assessment of sample storage techniques for total alkalinity and dissolved inorganic carbon in seawater, Limnol. Oceanogr.-Meth., 10, 711–717, 2012.

Huang, W.-J., Cai, W.-J., Wang, Y., Lohrenz, S. E., Murrell. M. C.: The carbon dioxide system on the Mississippi River-dominated continental shelf in the northern Gulf of Mexico: 1. Distribution and air-sea CO_2 flux, J. Geophys. Res-Oceans., 120, 1429-1445, 2015.

Hunt, C. W., Salisbury, J. C., Vandemark, D., and McGillis, W.: Contrasting Carbon Dioxide Inputs and Exchange in Three Adjacent New England Estuaries, Estuar. Coast, 34, 68-77, 2010.

Hunt, C. W., Salisbury, J. E., and Vandemark, D.: CO_2 input dynamics and air–sea exchange in a large New England estuary, Estuar. Coast, 37, 1078-1091, 2014.

Jiang, L.-Q., Cai, W.-J., and Wang, Y.: A comparative study of carbon dioxide degassing in river- and marine-dominated estuaries, Limnol. Oceanogr., 53, 2603–2615, 2008a.

Jiang, L.-Q., Cai, W.-J., Wanninkhof, R., Wang, Y., and Lüger, H.: Air-sea CO_2 fluxes on the U.S. South Atlantic Bight: spatial and seasonal variability, J. Geophys. Res., 113, C07019, doi:10.1029/2007JC004366, 2008b.

Ketchum, B. H.: The distribution of salinity in the estuary of the Delaware River, Woods Hole Oceanographic Institution, Woods Hole, Massachusetts, 1952.

Laruelle, G. G., Lauerwald, R., Rotschi, J., Raymond, P. A., Hartmann, J., and Regnier, P.: Seasonal response of air–water CO_2 exchange along the land–ocean aquatic continuum of the northeast North American coast, Biogeosciences, 12, 1447-1458, doi:10.5194/bg-12-1447-2015, 2015.

Lebo, M.L., L.A. Cifuentes, M.L. Fogel, M.P. Hoch, R.G. Keil, D.L. Kirchman, J.M. Ludlam, J.R. Pennock, J.H. Sharp, P.T. Spicer, and D.J. Velinsky.: Data from the Delaware Estuary Scenic Cruises. April 1986 – September 1988. Oceanographic Data Report Number 7. Del. Sea. Grant. Program, University of Delaware, Available from Sharp, J. H., 139 pp., 1990.

Mehrbach, C., Culberson, C. H., Hawley, J. E., and Pytkowicz, R. M.: Measurement of the apparent dissociation constants of carbonic acid in seawater at atmospheric pressure, Limnol. Oceanogr., 18, 897–907, 1973.

Millero, F. J., Graham, T. B., Huang, F., Bustos-Serrano, H., and Pierrot, D.: Dissociation constants of carbonic acid in seawater as a function of salinity and temperature, Mar. Chem., 100, 80–94, 2006.

McGillis, W. R., Edson, J. B., Hare, J. E., and Fairall, C. W.: Direct covariance air-sea CO_2 fluxes, J. Geophys. Res-Oceans., 106, 16729-16745, 2001.

McGillis, W. R., Edson, J. B., Zappa, C. J., Ware, J. D., McKenna, S. P., Terray, E. A., Hare, J. E., Fairall, C. W., Drennan, W., Donelan, M., DeGrandpre, M. D., Wanninkhof, R., and Feely, R. A.: Air-sea CO_2 exchange in the equatorial Pacific, J. Geophys. Res-Oceans., 109, 1978-2012, 2004.

Neubauer, S. and Anderson, I. C.: Transport of dissolved inorganic carbon from a tidal freshwater marsh to the York River estuary, Limnol. Oceanogr., 48, 299–307, 2003.

Pennock, J. R.: Temporal and spatial variability in phytoplankton ammonium and nitrate uptake in the Delaware Estuary, Estuar. Coast. Shelf. S., 24, 841-857, 1987.

Pierrot, D., Lewis, E., and Wallace, D. W. R.: CO2SYS DOS Program Developed for CO2System Calculations. ORNL/CDIAC-105., Carbon Dioxide Information Analysis Center, Oak RidgeNational Laboratory, US Department of Energy, Oak Ridge, California, 2006.

Raymond, P. A. and Cole, J. J.: Gas exchange in rivers and estuaries: choosing a gas transfer velocity, Estuaries, 24(2), 312–317, 2001.

Raymond, P. A., Caraco, N. F., and Cole, J. J.: Carbon dioxide concentration and atmospheric flux in the Hudson River, Estuaries, 20, 381-390, 1997.

Raymond, P. A., Bauer, J. E., and Cole, J. J.: "Atmospheric CO_2 evasion, dissolved inorganic carbon production, and net heterotrophy in the York River estuary, Limnol. Oceanogr., 45, 1707-1717, 2000.

Regnier, P., Friedlingstein, P., Ciais, P., Mackenzie, F. T., Gruber, N., Janssens, I. A., Laruelle, G. G., Lauerwald, R., Luyssaert, S., Andersson, A. J., Arndt, S., Arnosti, C., Borges, A. V., Dale, A. W., Gallego-Sala, A., Godderis, Y., Goossens, N., Hartmann, J., Heinze, C., Ilyina, T., Joos, F., LaRowe, D. E., Leifeld, J., Meysman, F. J. R., Munhoven, G., Raymond, P. A., Spahni, R.,

Suntharalingam, P., and Thullner, M.: Anthropogenic perturbation of the carbon fluxes from land to ocean, Nature Geosci., available online at: doi:10.1038/ngeo1830, 2013.

Salisbury, J. E., Vandemark, D., Hunt, C. W., Campbell, J. W., McGillis, W. R., and McDowell, W. H.: Seasonal observations of surface waters in two Gulf of Maine estuary-plume systems: Relationships between watershed attributes, optical measurements and surface pCO_2, Estuar. Coast. Shelf. S., 77, 245-252, 2008.

Sharp, J. H.: The Delaware Estuary: Research as background for estuarine management and development, Univ. Delaware Sea Grant College Program, p. 79-118, 1983.

Sharp, J. H.: Estuarine oxygen dynamics: What can we learn about hypoxia from long-time records in the Delaware Estuary? Limnol. Oceanogr., 55, 535-548, 2010.

Sharp, J. H., Yoshiyama, K., Parker, A. E., Schwartz, M. C., Curless, S. E., Beauregard, A. Y., Ossolinski, J. E., and Davis, A. R.: A biogeochemical view of estuarine eutrophication: seasonal and spatial trends and correlations in the Delaware Estuary, Estuar. Coast, 32, 1023-1043, 2009.

Sheldon, J. E. and Merryl, A.: A comparison of residence time calculations using simple compartment models of the Altamaha River Estuary, Georgia, Estuaries, 25, 1304-1317, 2002.

Takahashi, T., Ólafsson, J., Goddard, J. G., Chipman, D. W., and Sutherland, S. C.: Seasonal variation of CO_2 and nutrient salts over the high latitude oceans: A comparative study, Global Biogeochem. Cy., 7, 843–878, 1993.

Takahashi, T., Sutherland, S. C., Sweeney, C., Poisson, A., Metzl, N., Tilbrook, T., Bates, N., Wanninkhof, R., Feely, R. A., Sabine, C., Olafsson, J., and Nojiri, Y.: Global sea-air CO_2 flux based on climatological surface ocean pCO_2, and seasonal biological and temperature effects, Deep-Sea Res. Pt. II, 49, 1601–1622, 2002.

Trabalka, J. R. and Reichle, D. E.: The changing carbon cycle: A global analysis, Springer, New York, 2013.

Voynova, Y. G. and Sharp, J. H.: Anomalous biogeochemical response to a flooding event in the Delaware Estuary: a possible typology shift due to climate change, Estuar. Coast, 35, 943-958, 2012.

Wang, Z. A. and Cai, W.-J.: Carbon dioxide degassing and inorganic carbon export from a marsh-dominated estuary (the Duplin River): A marsh CO_2 pump. Limnol. Oceanogr., 49, 341-354, 2004.

Wang, Z. A., Cai, W.-J., Wang, Y., and Upchurch, B. L.: A long pathlength liquid-core waveguide sensor for real-time pCO_2 measurements at sea, Mar. Chem., 84, 73-84, 2003.

Wanninkhof, R.: Relationship between wind speed and gas exchange over the ocean, J. Geophys. Res-Ocean., 97, 7373–7382, doi:10.1029/92jc00188, 1992.

Wanninkhof, R.: Relationship between wind speed and gas exchange over the ocean revisited, Limnol. Oceanogr-Meth., 12, 351-362, 2014.

Wanninkhof, R., Doney, S. C., Takahashi, T., and McGillis, W. R.: The effect of using time-averaged winds on regional air-sea CO_2 fluxes, in: Gas transfer at water surfaces. Geophysical Monograph Series, edited by: Donelan, M., Drennan, W., Saltzman, E., and Wanninkhor, R., AGU, Washington D.C., 351-357, 2002.

Wanninkhof, R., Asher, W. E., Ho, D. T., Sweeney, C., and McGillis, W. R.: Advances in quantifying air-sea gas exchange and environmental forcing, Ann. Rev. Mar. Sci., 1, 213-244, 2009.

Weiss, R. F.: Carbon dioxide in water and seawater: the solubility of non-ideal gas, Mar. Chem., 2, 221–231, 1974.

Yoshiyama, K. and Sharp, H. J.: Phytoplankton response to nutrient enrichment in an urbanized estuary: Apparent inhibition of primary production by overeutrophication, Limnol. Oceanogr., 51, 424-434, 2006.

Zappa, C. J., McGillis, W. R., Raymond, P, A., Edson, J. B., Hintsa, E. J., Zemmelink, H. J., Dacey, J. W. H., and Ho, D. T.: Environmental turbulent mixing controls on air-water gas exchange in marine and aquatic systems, Geophys. Res. Lett., 34, 2007.

Table 1. Averaged temperature coefficients [($\partial \ln pCO_2/\partial T$)/$pCO_2$] for each salinity bin. Simulated surface water pCO_2 values at varying salinities were computed using river and ocean end-member TA and DIC values of 900 and 960 μmol kg-1 and 2300 and 2000, respectively.

Salinity	Coefficient
0 – 5	0.0332
5 – 10	0.0382
10 – 15	0.0411
15 – 20	0.0417
20 – 25	0.0417
25 – 30	0.0415
30 – 35	0.0420

Table 2. Area-averaged, standard deviation, and range of pCO_2 and CO_2 flux (F_{CO2}) in five of the six zones in the Delaware Estuary during each cruise.

		Mar 2014	Jun 2013	Jul 2014*	Aug 2013*	Aug 2014	Oct 2013*	Oct 2014	Nov 2013	Dec 2014*	Annual Average
Average pCO_2 (µatm)											
Lower Bay	Mean ± SD	230 ± 23	477 ± 11	473 ± 52	384 ± 42	315 ± 59	421 ± 6	405 ± 8	387 ± 3	596 ± 11	410
	Range	194 – 267	456 – 528	397 – 648	317 – 491	243 – 432	413 – 437	395 – 419	380 – 393	570 – 627	
Mid-Bay	Mean ± SD	198 ± 8	540 ± 66	559 ± 97	530 ± 36	250 ± 16	465 ± 22	422 ± 2	390 ± 8	590 ± 21	438
	Range	187 - 232	464 – 759	402 – 777	464 – 607	223 – 310	429 – 516	417 – 431	378 – 415	566 – 654	
Upper Bay	Mean ± SD	289 ± 47	919 ± 192	917 ± 97	680 ± 58	470 ± 98	566 ± 39	463 ± 19	434 ± 11	658 ± 26	599
	Range	225 - 401	645 – 1374	768 – 1149	594 – 846	312 – 697	508 – 651	428 - 483	411 – 461	597 – 744	
Turbidity	Mean ± SD	595 ± 121	2087 ± 499	1473 ± 162	1237 ± 139	1102 ± 317	726 ± 34	575 ± 79	542 ± 61	786 ± 39	1014
Maximum Zone	Range	397 - 854	1327 – 2981	1141 – 1680	837 – 1370	689 – 1866	645 – 754	481 – 737	457 – 709	711 – 1000	
Urban River	Mean ± SD	868 ± 48	3287 ± 163	2994 ± N/A	2542 ± N/A	2310 ± 589	1199 ± N/A	816 ± 133	880 ± 179	878 ± N/A	1753
	Range	762 – 945	3007 – 3600	N/A	N/A	1822 – 4000	N/A	640 – 1330	615 – 1450	N/A	
Average F_{CO2} (mmol m^{-2} d^{-1})											
Lower Bay	Mean ± SD	-15.4 ± 2.3	3.8 ± 0.5	4.4 ± 2.5	3.8 ± 1.9	-3.0 ± 2.7	1.6 ± 0.4	0.8 ± 0.6	-1.2 ± 0.3	13.5 ± 1.0	0.9
	Range	-19.4 - (-12.0)	2.8 – 6.2	0.5 – 13.1	0.8 – 8.5	-6.4 – 2.5	1.1 – 2.6	0.1 – 1.8	-1.9 – (-0.7)	11.6 – 15.7	
Mid-Bay	Mean ± SD	-20.0 ± 0.6	6.8 ± 3.2	11.1 ± 6.8	10.2 ± 1.6	-6.7 ± 0.7	4.8 ± 1.8	2.0 ± 0.1	-1.1 ± 0.7	13.5 ± 2.0	2.3
	Range	-21.0 - (-17.8)	3.2 – 17.4	0.8 – 27.8	7.3 – 13.6	-8.0 – (-3.9)	2.1 – 9.0	1.6 – 2.7	-2.1 – 1.3	11.2 – 19.3	
Upper Bay	Mean ± SD	-12.1 ± 4.9	25.3 ± 9.5	39.5 ± 7.3	16.8 ± 2.6	5.7 ± 6.0	13.0 ± 2.9	5.0 ± 1.4	3.4 ± 1.2	19.7 ± 2.0	12.9
	Range	-18.4 – (-0.5)	11.8 – 48.0	26.9 – 54.7	13.0 – 24.3	-3.8 – 19.0	8.4 – 18.6	2.5 – 6.5	0.9 – 5.9	14.2 – 25.1	
Turbidity	Mean ± SD	15.9 ± 9.6	83.9 ± 25.2	63.5 ± 2.9	42.2 ± 6.9	37.1 ± 13.9	21.1 ± 0.9	12.3 ± 5.1	10.1 ± 3.0	26.7 ± 1.9	34.8
Maximum Zone	Range	-0.9 – 36.9	45.6 – 129.1	54.3 – 65.5	23.9 – 47.6	18.6 – 71.9	18.3 – 21.7	6.3 – 23.6	5.6 – 19.7	23.3 – 44.8	
Urban River	Mean ± SD	38.3 ± 4.3	144.8 ± 8.1	131.0 ± N/A	109.8 ± N/A	98.9 ± 25.9	52.1 ± N/A	30.2 ± 8.6	31.0 ± 8.1	32.1 ± N/A	74.2
	Range	33.6 – 45.5	130.4 – 160.0	N/A	N/A	83.0 – 175.4	N/A	17.8 – 64.1	20.9 – 66.4	N/A	

*Months when surveys did not extend into Urban River. Area-averaged was estimated by linearly regressing data from adjacent months with sample measurements. Standard deviation and range not available.

1 Table 3. Flushing time in five of the six zones in the Delaware Estuary during each cruise.

	Mar 2014	Jun 2013	Jul 2014	Aug 2013	Aug 2014	Oct 2013	Oct 2014	Nov 2013	Dec 2014	Annual Average
Flushing Time (day)										
Lower Bay	14.5	11.7	26.5	23.8	36.2	21.9	18.5	21.9	16.1	21.2
Mid-Bay	29.9	22.9	54.5	38.1	64.1	41.3	30.9	40.0	28.3	38.9
Upper Bay	15.1	13.3	26.6	23.9	32.8	25.5	27.6	27.2	16.6	23.2
Turbidity Maximum Zone	7.6	7.5	11.9	13.3	18.5	19.9	16.1	16.9	11.3	13.7
Urban River	2.5	2.3	3.7	6.1	6.9	6.5	6.5	6.5	5.9	5.2

2

Table 4. Calculated $\Delta pCO_{2thermal}$, $\Delta pCO_{2non\text{-}thermal}$, $T - B$, and T/B values for each salinity interval in the Delaware Estuary.

	0-5	5-10	10-15	15-20	20-25	25-30
$\Delta pCO_{2thermal}$ (µatm)	1005	800	635	514	417	431
$\Delta pCO_{2non\text{-}thermal}$ (µatm)	773	477	615	635	604	473
$T - B$ (µatm)	232	323	20	-121	-187	-42
T/B	1.30	1.68	1.03	0.80	0.69	0.91

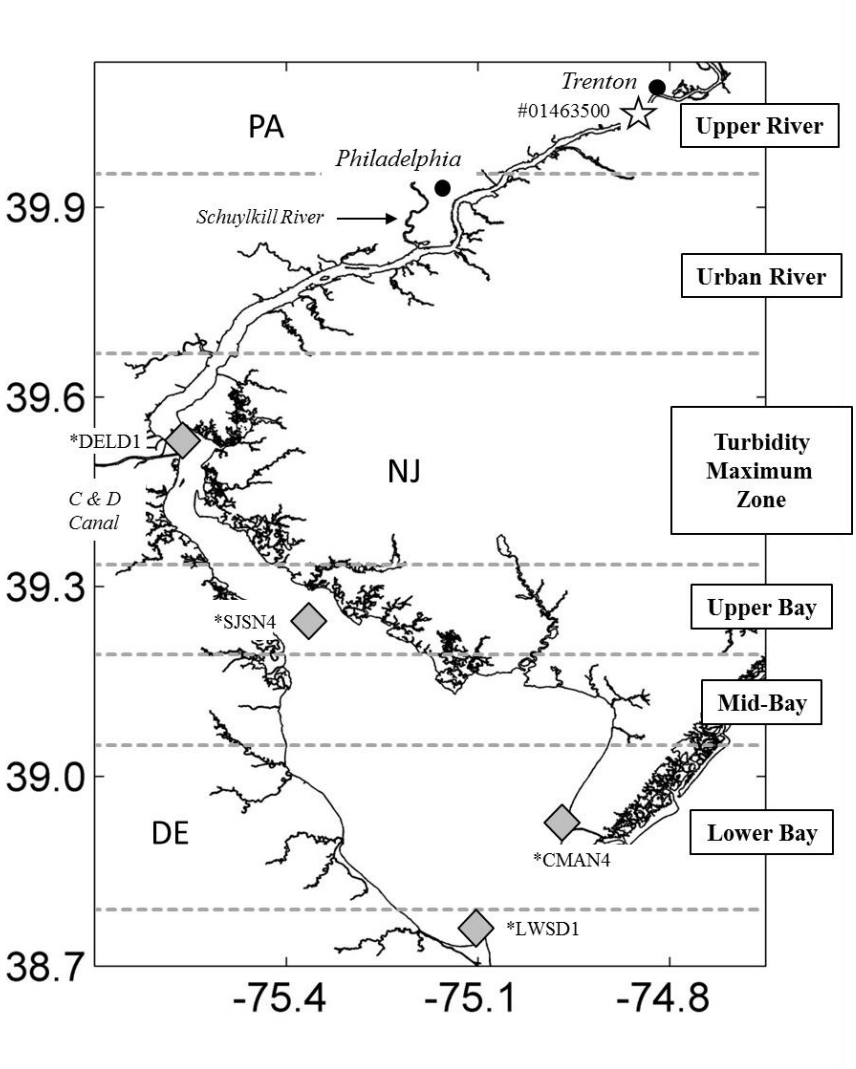

Figure 1. Map of the Delaware Estuary divided into six zones from the head of the tide in Trenton, NJ to the mouth of the bay as defined in Sharp et al. (2009). The gray diamonds indicate the position of four NOAA buoys (LWSD1, CMAN4, SJSN4, and DELD1). The white star shows the location of the USGS gauging station (#01463500).

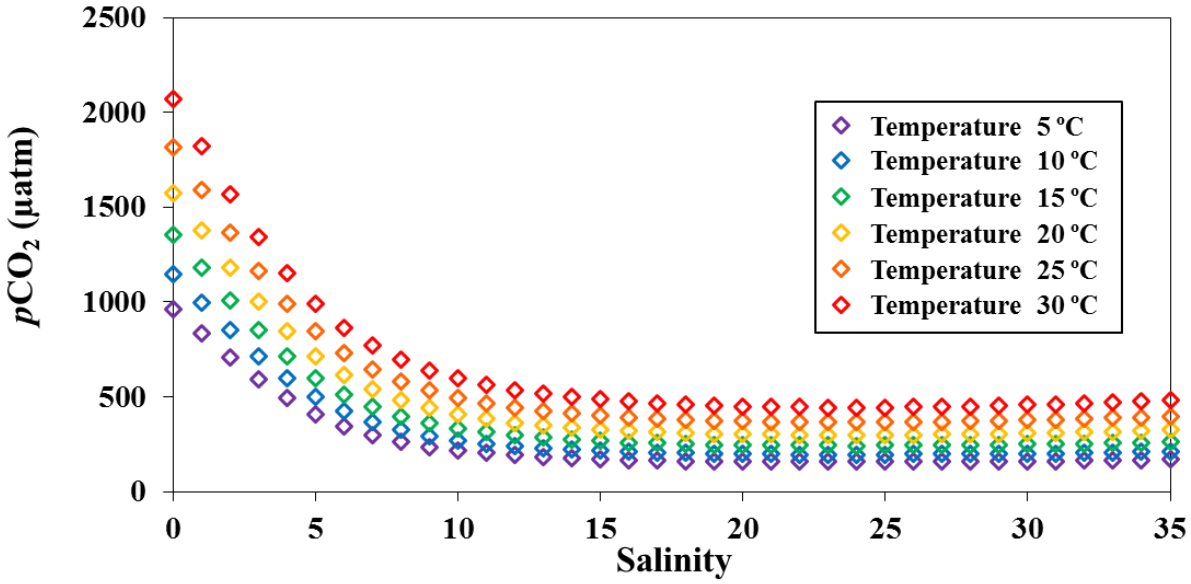

Figure 2. Simulated surface water pCO_2 against salinity grouped by temperature bins. Surface water pCO_2 values were calculated using river and ocean end-member TA and DIC values of 900 and 960 µmol kg^{-1} and 2300 and 2000 µmol kg^{-1}, respectively.

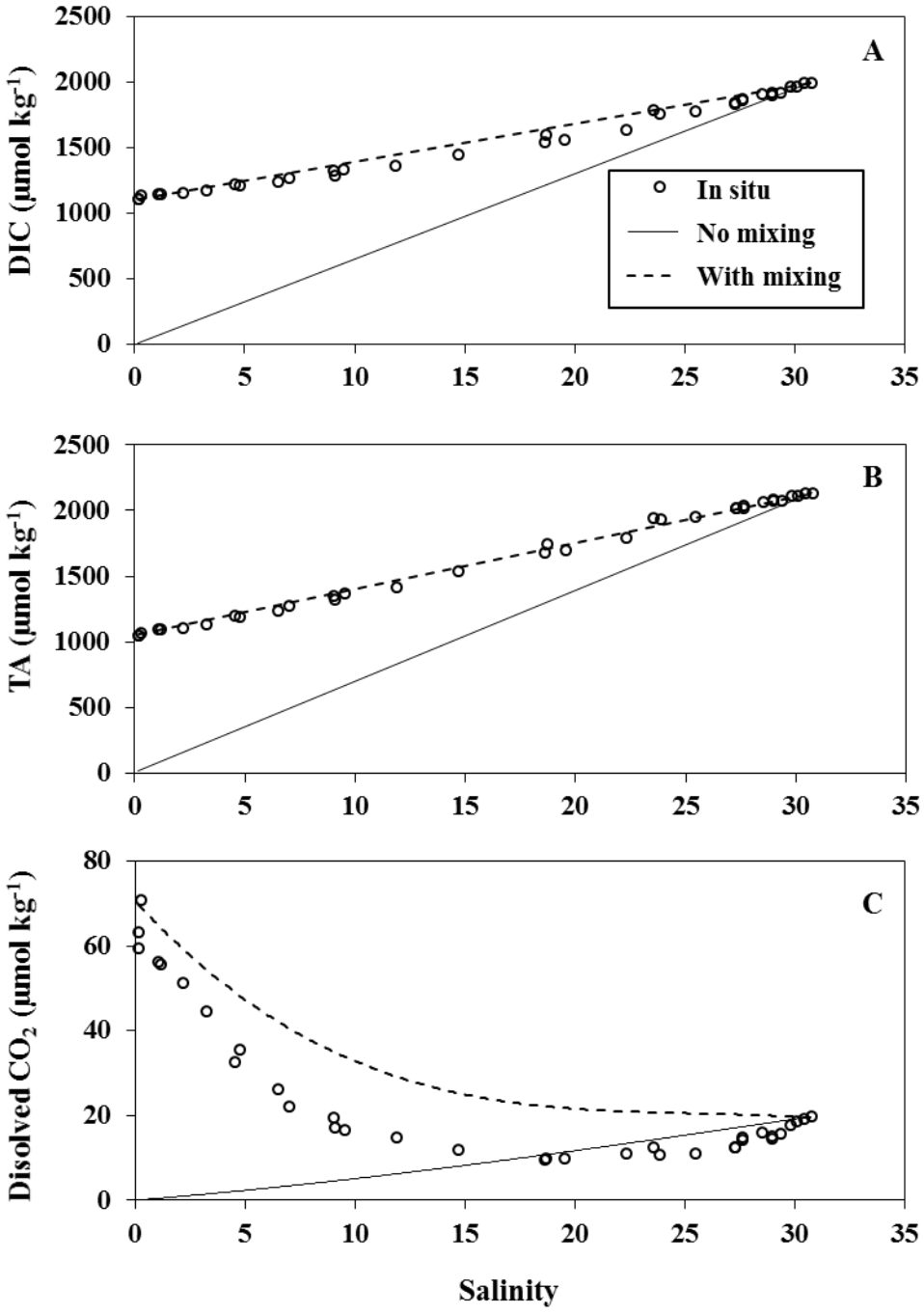

Figure 3. Concentrations of (A) DIC, (B) TA, and (C) dissolved CO_2 in the Delaware Estuary during March 2014. Open circles represent in situ concentrations. Solid lines represent values after the ocean end-member is diluted by freshwater with a concentration of zero units. Dotted lines represent concentration after mixing of river and ocean end-members. CO2SYS was used to calculate pCO_2 from measured DIC and TA.

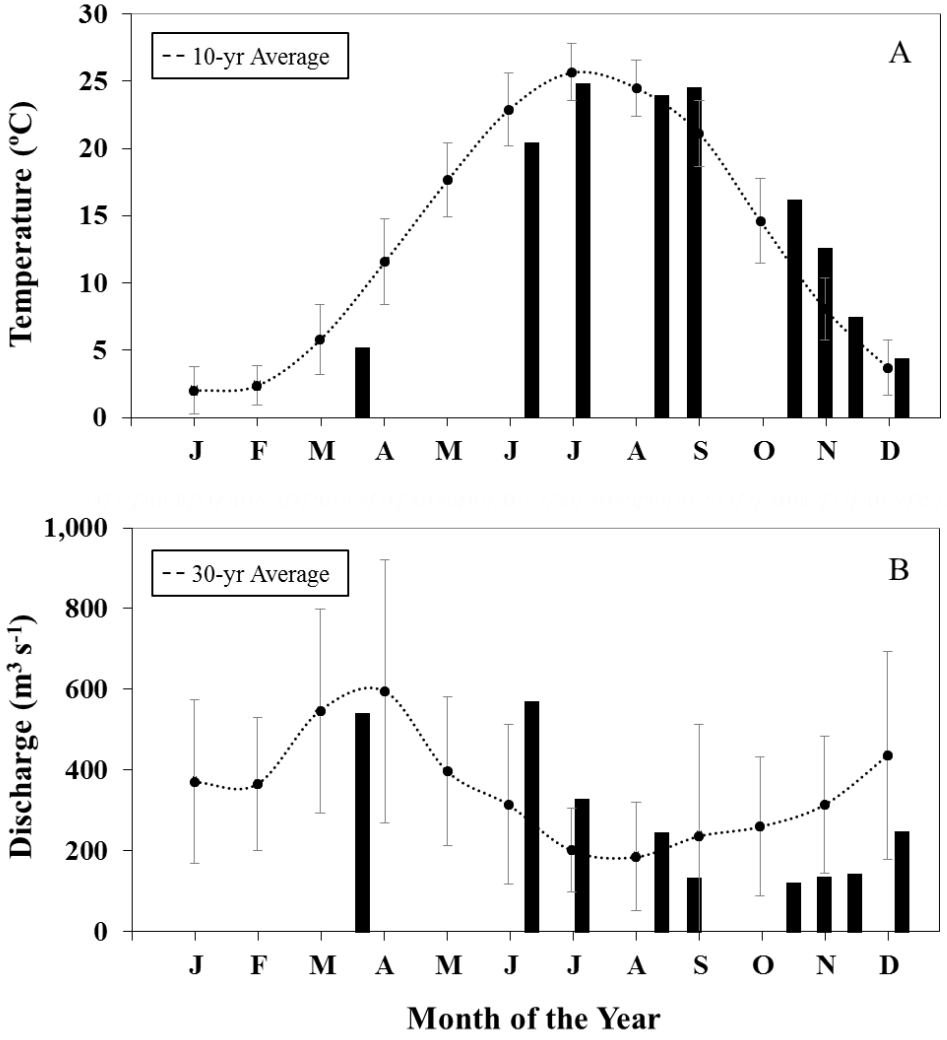

Figure 4. (A) Surface water temperatures and (B) Delaware River discharge rates recorded in the Delaware Estuary during each sampling month. Error bars represent standard deviations of the 10-year (2004-2014) and 30-year (1980-2014) monthly averages for surface water temperatures and Delaware River discharge rates, respectively.

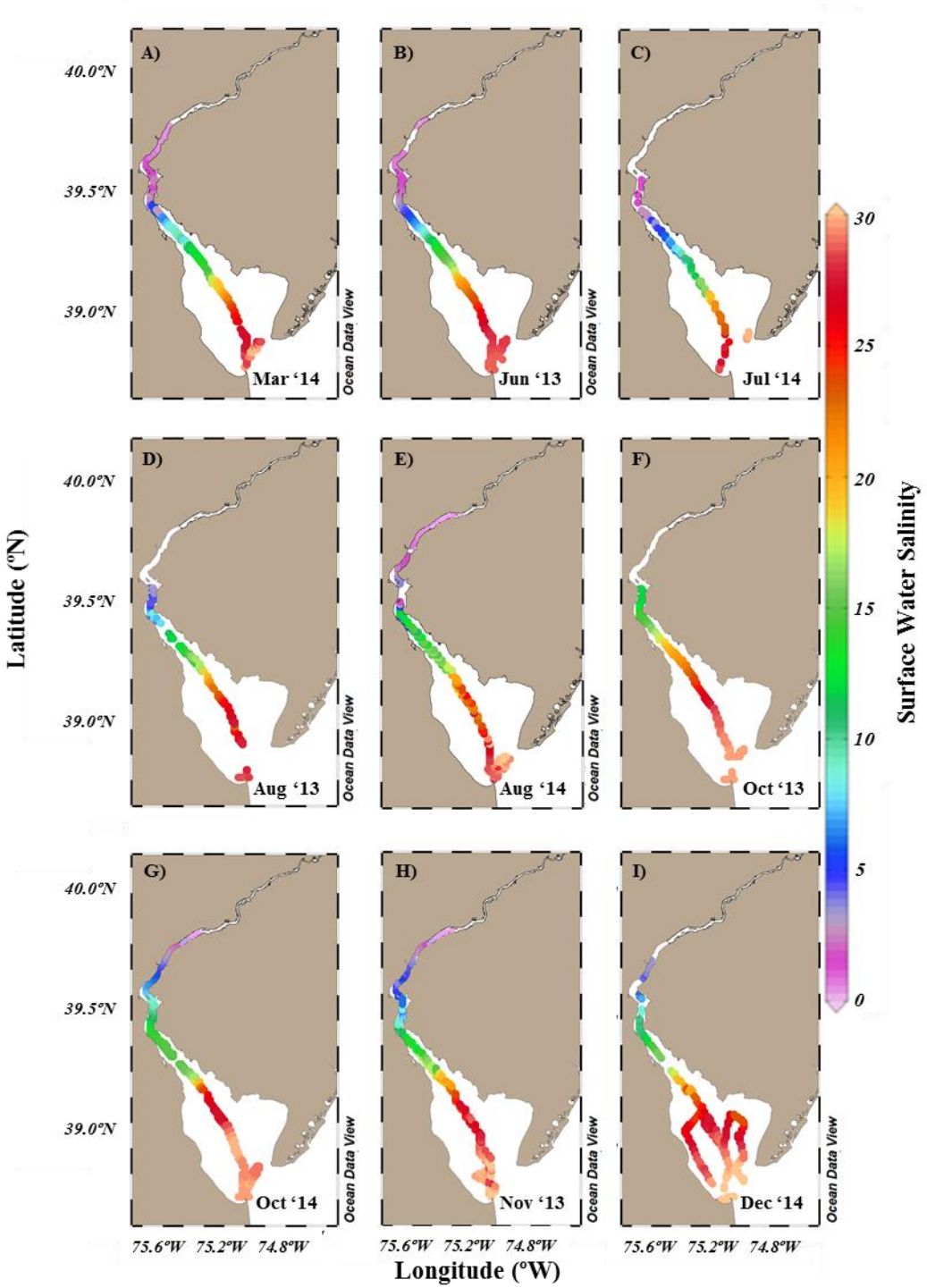

Figure 5. Spatial distributions of surface water salinity in the Delaware Estuary measured during each sampling month. The map was designed with the ODV software by R. Schlitzer (Ocean Data View software, 2015, http://odv.awi.de/.

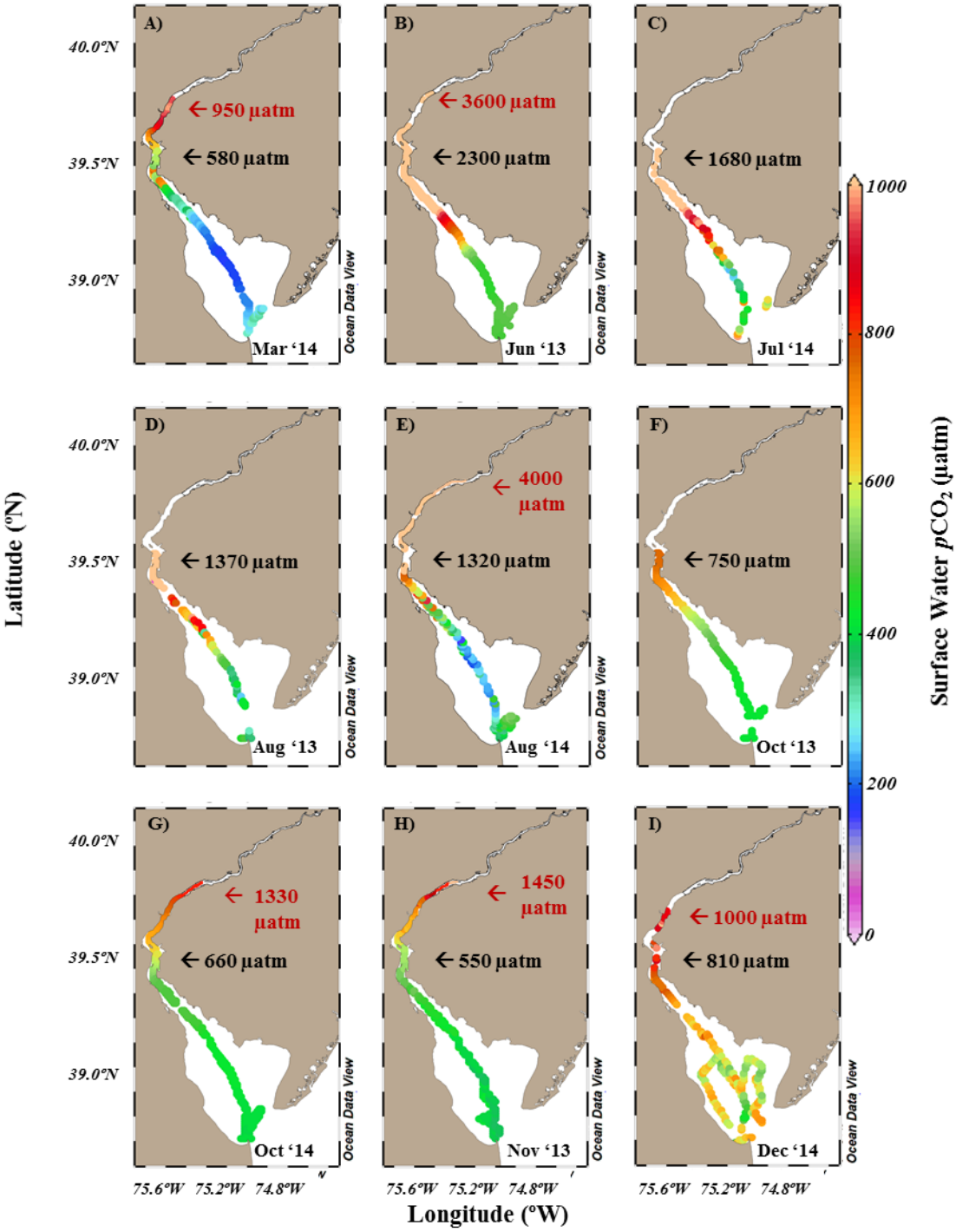

Figure 6. Spatial distributions of surface water pCO_2 in the Delaware Estuary measured during each sampling month. Black and red arrows show surface water pCO_2 values at the Chesapeake-Delaware Canal and the northern end member of each survey, respectively. The map was

designed with the ODV software by R. Schlitzer (Ocean Data View software, 2015, http://odv.awi.de/.

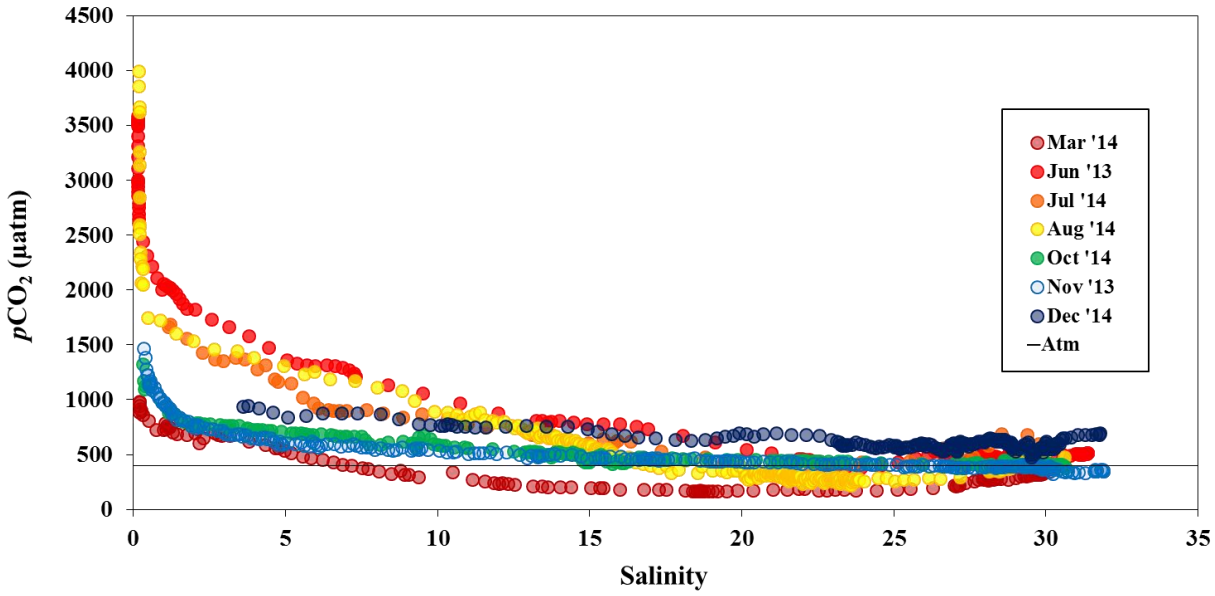

Figure 7. Measured surface water pCO_2 against the salinity gradient during each sampling month in the Delaware Estuary.

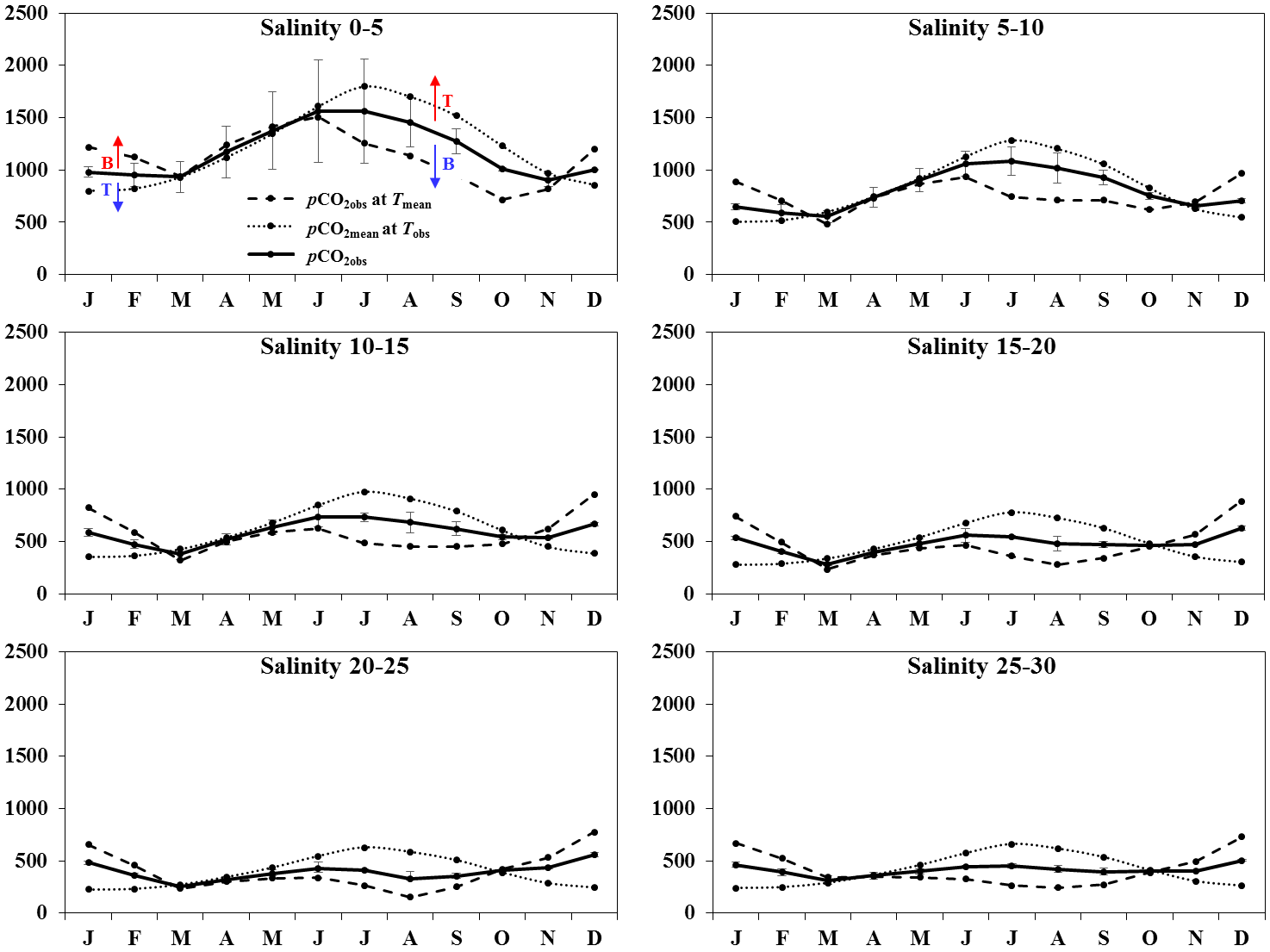

Figure 8. Salinity-binned intervals of temperature-normalized observed pCO_2 values at 13.3 ºC, annual mean, area-averaged pCO_2 values at in situ temperature, and observed pCO_2 values in the Delaware Estuary over the year. Red arrows indicate increases in pCO_2 and blue arrows indicate decreases in pCO_2. The symbol T represents changes in pCO_2 due to thermal processes and the symbol B represents fluctuations in pCO_2 due to non-thermal processes. Error bars represent one standard deviation of the mean value for each month.

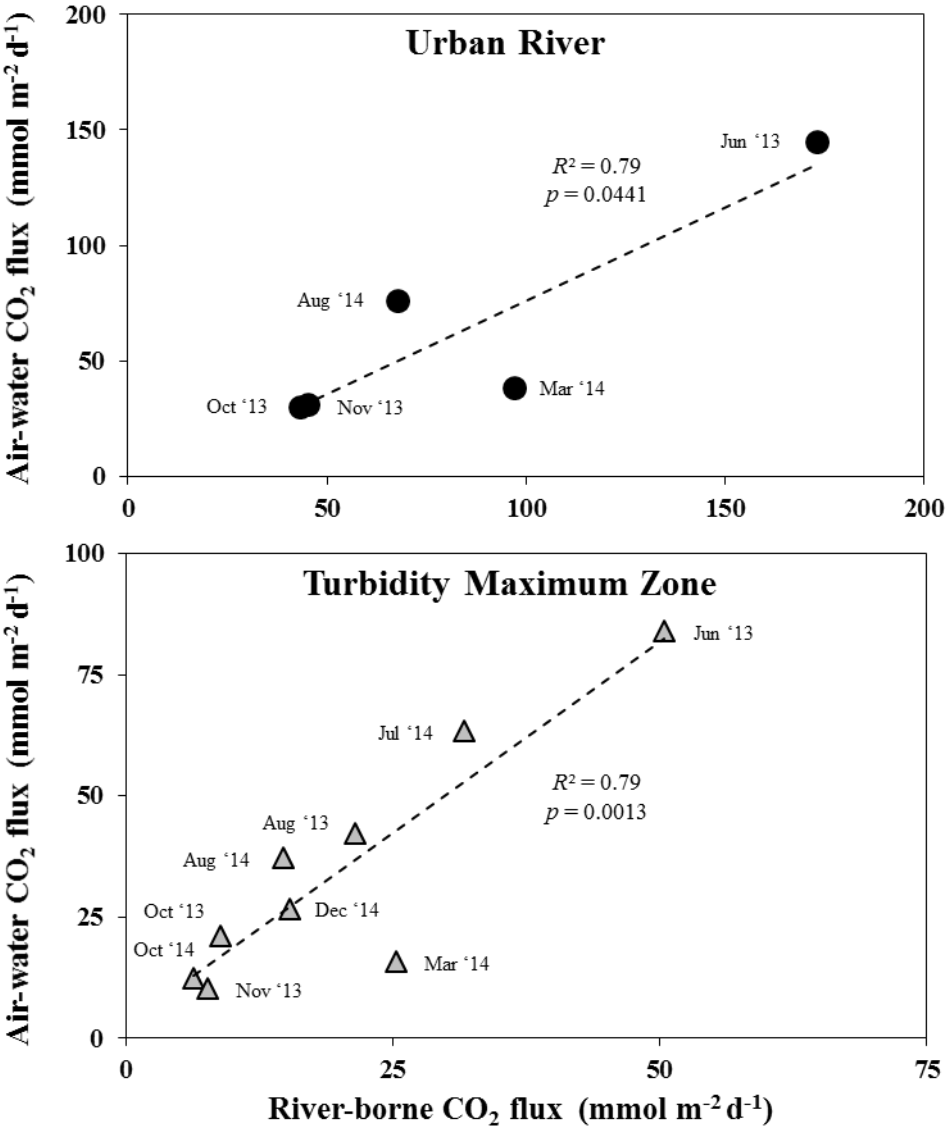

Figure 9: Air-water CO_2 fluxes against river-borne CO_2 fluxes in the urban river and turbidity maximum zone of the Delaware Estuary. Note the different axes used for the urban river and turbidity maximum zone.

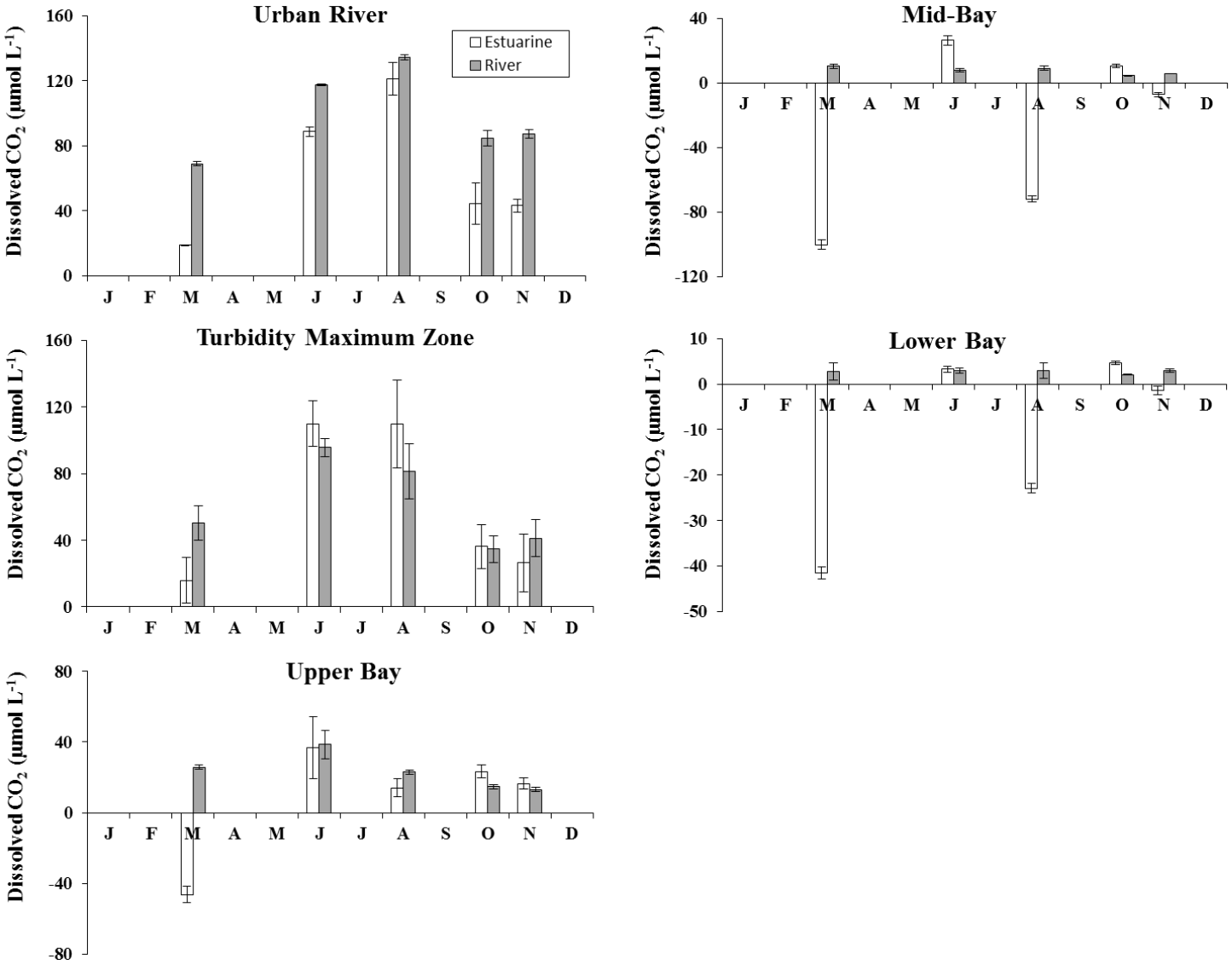

Figure 10: Dissolved CO_2 concentrations (normalized to 13.3 ºC, area-averaged) due to river inputs and internal estuarine sources in each region of the Delaware Estuary. Note the different axes used across all regions of the estuary. Error bars represent one standard deviation of the mean value for each month.